Aerosol route in Processing of Nanostructured Functional Materials[†]

O. Milosevic[*1], L. Mancic[1], M. E. Rabanal[2], L. S. Gomez[2], K. Marinkovic[1]
Institute of Technical Sciences of the Serbian Academy of Sciences and Arts [1]
Universidad Carlos III de Madrid[2]

Abstract

The diversity and potentials of the aerosol route for making functional materials at the nano size level are reviewed. Among the methods currently used for nanophase processing, synthesis through dispersion phase (aerosol) enables generation of ultrafine, either single or complex powders with controlled stoichiometry, chemical and phase content provided by high surface reaction, high heating and cooling rates and short residence time. It represents a "bottom-up" chemical approach and provides control over a variety of important parameters for particle processing. This may favors to the formation of either amorphous, nanocrystalline or metastable phases implying a huge impact in the search for advanced functional materials having novel and unique structures and properties. Particularly, the opportunities of the hot wall aerosol synthesis, i.e. spray pyrolysis, for the generation of ultrafine spherical particles with uniformly distributed components, phases and nano-clustered inner structure and luminescence properties is demonstrated with various analyzing techniques like XRPD, FE-SEM, HR-TEM, STEM and nanotomography. Following the initial attempts, a more detailed aspect of the several phosphor particles generation based on Gd_2O_3:Eu, Y_2O_3:Eu, $(Y_{1-x}Gd_x)_2O_3$:Eu and $Y_3Al_5O_{12}$:Ce is reviewed highlighting the research activities in the Institute of Technical Sciences of SASA, Serbia.

Keywords: aerosol, nanoparticles, synthesis, phosphors, luminescence

1. Introduction

Tremendous technological and scientific trend in material science for miniaturization and microstructure refinement is basically followed with the increasing interest for nanophase characterization and understanding. The field of nanoscience and nanotechnology has an exciting progress in recent years, particularly regarding the control synthesis of ultrafine particles or nanoparticles that might have a great potential for use in solid-state functional materials and devices, like phosphors, sensors, catalysts, drug delivery carriers etc.[1] The key points important for the future research and development of nanophased materials represent the ability for further improvement of material properties through nanostructuring and fundamental research of structure-properties relationship, from one side, as well as development of assigned and controlled synthesis route with the ability to ensure nanophase synthesis in a controlled manner, from another. Synthesis of submicronic and nanosized powders and thin films represent an area of increasingly high interest and offers new opportunities in materials engineering whether one or multi component systems are considered.

The chemical synthesis routes, like liquid precipitation, sol-gel or hydrothermal methods, offer many advantages over conventional procedures for nanoscaled materials processing. Since the precursors are mixed at the molecular level in a solution, a high degree of structural homogeneity is achievable; doping is effective, surface area of powder produced is very high, leading to lower processing temperature. Moreover, the solution routes and low temperature processing minimize the potential for contamination, which is very important for the most applications in the electronic, optoelectronic, chemical industries etc. that are sensitive to some of the impurities. Compared to other processing techniques, powder

synthesis through aerosol routes enable the generation of fine, submicronic to nanoscale, either single or complex, powders from a variety of precursor solutions[2-6]. It represents basically chemical route having a "bottom-up" approach for powder processing. The diversity of aerosol routes, depending mainly on the nature of aerosol and the manner how the aerosol decomposition energy is transferred to the system are presented on **Fig.1**. Two cases are roughly evident in aerosol routes: gas-to-particle route, which relates to the particle formation from the gaseous precursors and droplet-to-particle route, that relates to the formation of discreet aerosol droplets and control of the aerosol decomposition into particles[3]. Depending on how the thermal energy is provided to the precursors, affecting the most important particle formation parameters: residence time and temperature distribution, the main aerosol decomposition methods could be presented as is on **Fig.1**. The advantages of aerosol synthesis are as follows: it represents a simple method for production of oxide, non-oxide, metal and composite powders of complex composition, either in amorphous, crystalline or nanocrystalline state. Solution chemistry approaches offer design of materials at the molecular level, spherical particle morphology with full or hollow spheres, with narrow particle size distribution and a very homogeneous composition can be achieved by properly adjustment of the process parameters. For the case of film processing, this method provides easy control of deposition rate and thickness, simple doping of films using any element in any proportion by addition of a suitable dopant into the starting solution, possible production of layered films and films with concentration gradient, vacuum not required in any step of the process and there are no limits concerning dimensions and shape of substrate.

In the case of hot-wall processing[2-5,7-10], energy source for reaction and particle formation is usually provided through tubular flow reactor, flame synthesis use combustion enthalpy of vapor flame[11-13], self sustaining flame reactors use combustion enthalpy of dispersed oil phase in the form of emulsion[14], self combustion aerosol synthesis use combustion enthalpy of entire solution being chemically modified[15,16]. Tubular hot-wall flow reactor provide a well-controlled temperature profile over long residence times, while in the case of flame synthesis the decomposition temperatures are higher and the residence time is shorter. In aerosol assisted thin film preparation (Pyrosol process) there is precursor decomposition in the vicinity on the heated substrate[17-19]. Under certain circumstances, Pyrosol could be assimilated to a chemical vapor deposition process, but it removes restrictions of CVD such as high vapor pressure of precursors and their good thermal stability. In comparison to the pneumatic atomizers, the aerosol produced by ultrasonic atomization enables better controlling of droplet size and size distribution.

2. Hot-Wall Aerosol Synthesis (Spray pyrolysis)

Hot-wall aerosol synthesis is based on the formation of aerosols of precursor solutions and control over the aerosol decomposition in a high temperature tubular flow reactor through the successive processes of droplet evaporation, drying, solute precipitation and decomposition. Since the heterogeneous gas/liquid-solid reaction occurs in a dispersed system-aerosol at the level of few micrometers sized droplets, compositional segregation is prevented and high heating rates (20-300℃/s), as well as high surface
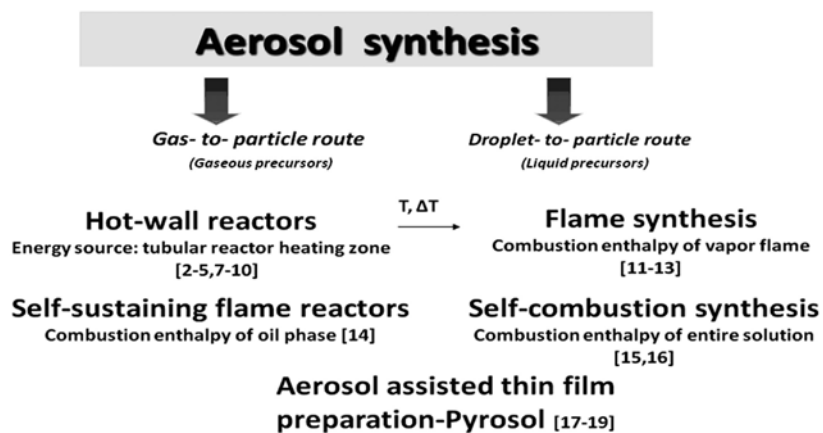
Fig. 1 The diversity of the aerosol routes, depending on the nature of aerosol (upper) and the manner of how the aerosol decomposition energy is provided to the system (down).

reaction could be achieved[2]. During decomposition, the aerosol droplets undergo evaporation/drying, precipitation and thermolysis in a single-step process. Consequently, spherical, solid, agglomerate-free, either submicronic, nanostructured or nanoscaled particles are obtained through the mechanisms of primary nano- particles coalescence, collision and sintering. Schematic of the hot-wall aerosol synthesis routes is presented in **Fig. 2**. The process involves formation of discreet droplets of precursor solution in the form of aerosol and control over their thermally induced decomposition and phase transformation.

Synthesis I refers to the chemical synthesis and solution preparation that could be in the form of true solutions, colloids or emulsions. In addition, the modification of the chemistry of the solution, i.e. additives like glycine, urea, suchrose etc. alters the morphology of the particles derived as well as the particle size, size distribution and agglomeration state. The precursors and precursors chemistry are usually characterized for their physico-chemical properties like determination of the solution surface tension, viscosity, density, concentration, pH, as well as the decomposition behavior of the precursors since there is a strong relationship between the mentioned solution properties and the droplet/particle size[21,22].

Aerosol is most frequently formed ultrasonically, using high-frequency (100KHz - 10MHz) ultrasonic beam[17] directed to the gas-liquid interface. Liquid atomization and aerosol formation occur for the certain values of the acoustic waves amplitude, where the average droplet size depends mostly on the solution properties (viscosity, surface tension, concentration, density etc.) as well as the ultrasound frequency. It was already shown that this technique is suitable for the aerosol formation with the narrow size of droplet distribution, thus affecting narrow particle size distribution.

Depending on the atomization technique, either monodispersed or polydispersed particles could be obtained. The monodispersed nano particles are formed either through the evaporation-condensation mechanisms, using electrospray atomizer or differential mobility classifier[23,24]. Twin-fluid and ultrasonic atomization techniques usually led to the formation of polydispersed particles. The droplet size and size distribution depend on the type of atomization and the precursor properties, as presented in **Table 1**.

The particle size is then defined by the following equation for the case that one particle is derived from one droplet[22]:

$$D_p = D_d \left(\frac{c^* M_s}{\rho_p M_p} \right)^{1/3} \tag{1}$$

Where: D_p- particle diameter [μm], c^*- initial solution concentration [gcm^{-3}], M_s- molecular mass of resulting powder [gmol^{-1}], M_p- molecular mass of precursor [gmol-1], ρ_p- powder density [gcm^{-3}]

The aerosol is carried out by the flowing gas stream into high-temperature tubular flow reactor. Differential mobility analyzer (DMA) or Scanning Mobility Particle Sizer (SMPS) can be used for on-line determination of the aerosol-born particle's size, size distribution and concentration[24].
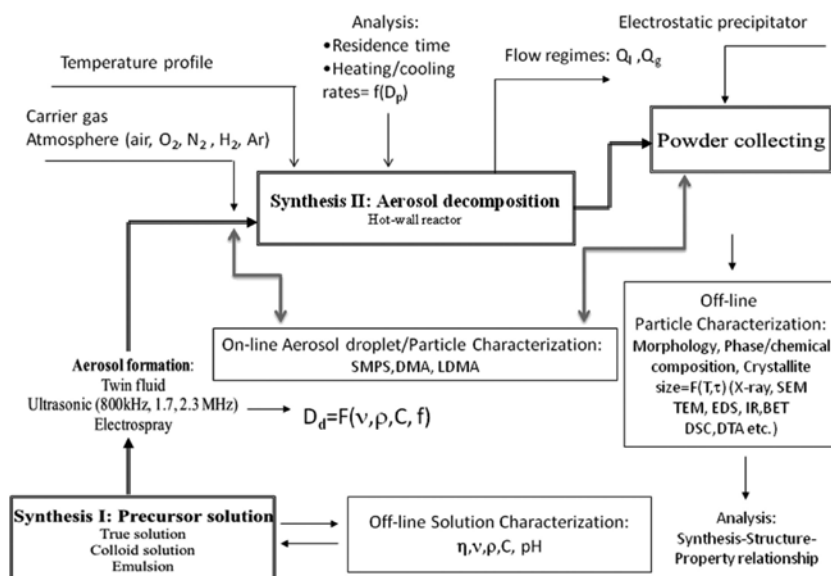
Fig. 2 Schematic of the hot-wall aerosol synthesis route methodology[20].

Table 1 The manner of the aerosol formation and droplet/particle size distribution

	Aerosol formation /Droplet size equations, μm
Monodispersed droplets/particles	Evaporation-Condensation [25]
	Electrospray aerosol route [23]
	Differential mobility classifier [24]
Polydispersed droplets/particles	Twin-fluid atomizationEmpirical relationship S.Nukiyama, Y.Tanasawa [26] ** $$D_d = \frac{585}{V}\left(\frac{\gamma}{\rho}\right)^{0.5} + 597\left(\frac{\mu}{(\gamma\rho)^{0.5}}\right)^{0.45}\left(\frac{1000F_L}{F_G}\right)^{1.5}$$
	Ultrasonic atomization Lang [21] *** $$D_d = 0.34\left(\frac{8\pi\gamma}{\rho f}\right)^{1/3}$$

** D_d- droplet diameter [μm]; V- relative carrier gas- to -liquid velocity at the nozzle exit[ms^{-1}]; γ - solution surface tension [10^3 Nm^{-1}] ; r- solution density [gcm^3]; μ - solution viscosity [Pas] ; F_G- gas flow rate [cm^{3}s^{-1}] ; F_L- liquid flow rate [cm^{3}s^{-1}]

*** D_d- droplet diameter [μm]; γ - solution surface tension [dyncm^{-1}]; r-solution density [gcm^3]; f - ultrasound frequency [10^3 s^{-1}]

The flow rate of the carrier gas represents one of the most important process parameters enabling the supporting atmosphere as well as the aerosol flow rate and the droplets residence time to be controlled. During the main process, denoted as *Synthesis II*, aerosol droplets undergo evaporation, drying and solute precipitation in a single-step process caused by the mechanisms of heat and mass transfer inside the droplets and between the droplets and surrounding gas. Such mechanism enables high surface reaction, solution stoichiometric retention as well as segregation suppression to the droplet scale. As a result, spherical, solid, agglomerate-free, either nano scale or submicronic particles are obtained having composite inner nano structure[27-34].

After solvent evaporation/drying stage and consecutively solute precipitation and decomposition that occurs at the droplet level, the primary particles arise through the thermally induced processes of nuclei formation, collision and coalescence. Resulting particles then arise through the growth and aggregation of nano scaled "primary particles" arranged in spherical so called "secondary particles". The secondary particle size and size distribution are mainly influenced by the properties of aerosol generator and precursor solutions. Primary particles, that represent either crystallites or block-mosaic assembles, sizing mainly below 50nm, could coalesced entirely or densified with existing nanoporosity and exhibiting high surface area. The Summary of the particle morphology hierarchy is presented at **Fig. 3**. The size of primary particles depends on the time-temperature history and materials properties. For low tempera-

tures and short residence time particle coalescence proceeds slowly compared to collisions, producing weak agglomerates having a high specific surface area. On the contrary, at high temperatures and for small particles, particle coalescence is dominant process resulting in primary particle growth, hard agglomerates and small specific surface area[35].

Nanophase particles can be generated in accordance to this method by properly controlling over the initial aerosol droplet size, the mechanisms of the droplet collision and coalescence as well as by suppressing the excessive grain growth and grain coarsening. As a result, it is possible to obtain either nanoparticles directly from nano-sized droplets or to obtain submicronic sized particles, that offer a composite nanograin particle structure[27, 34, 36]. **Fig. 4**. represents the methodology for directly producing of nanoscaled particles by spray pyrolysis. By following the proportionality of particle size with solution concentration and the droplet size (eq.1) and the basic concept of spray pyrolysis where one particle is derived from one droplet, directly producing of nano particles can be achieved from dilute solutions and small aerosol droplets[2]. Decrease of the droplet size can be achieved either by using electrospray atomizer, that is able to directly produce nanoscaled monodispersed particles or by the modification of the atomizing technique, like filter expansion aerosol generator (FEAG), developed for the synthesis of nanoscaled phosphor particles by low-pressure spray pyrolysis[23,36]. On the other hand, self combustion spray pyrolysis, associated with the modification of precursor chemistry by using of exothermic reacting
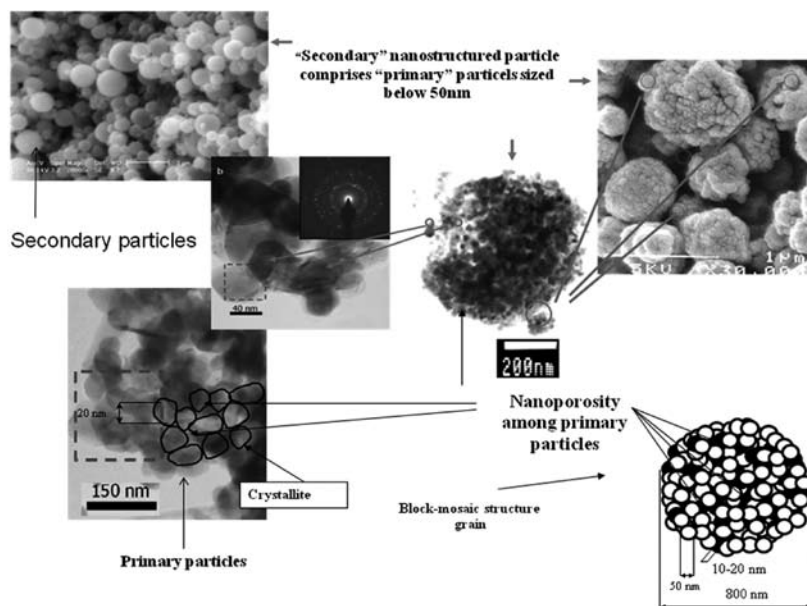
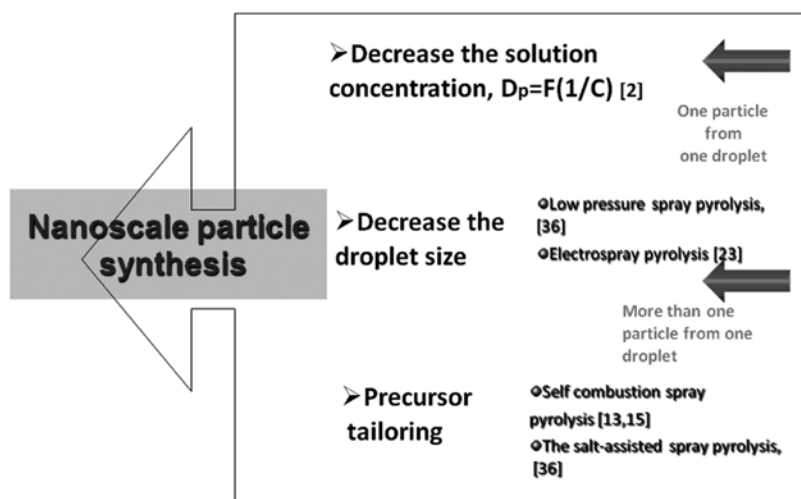**Fig. 3** Summary of the particle morphology hierarchy.

Fig.4 Nanoscale particle synthesis through aerosol route.

species, that cause droplets/particles to be decomposed with additional heat and exploding during the process, leads to the direct synthesis of nanoparticles[13,15].

The choice of precursors, their thermal and decomposition behavior play an important role in nanoscaled particles synthesis, as well[36,37]. The mechanisms of nucleation and growth of primary particles, ranging from few to several tens of nanometers, which gather together during decomposition process into spherical agglomerates, or so called "secondary particles" the mean size below 1000nm, play a crucial role in formation of particle size and morphology[15,38].

Salt assisted spray pyrolysis (SAD) enable releasing the nano-scaled primary particles by modification of the solution chemistry and preventing formation of hardly aggregated primary particles into the secondary particles[36].

From the viewpoint of the application of the as-generated particles for advanced materials synthesis, particle morphology is of great interest. Aerosol synthesis enables synthesis of various particle morphology, either as hollow or dense spheres. It is presumed that certain particle morphology is formed during the evaporation/drying stage that encountered processes of evaporation and diffusion of both the solvent, and

solute, changing in droplet temperature and crust formation. They are governed by the basic laws of heat and mass transfer so several models describing the above mentioned phenomena are developed and can be applied in prediction of particle morphology[39-41]. The problems regarding droplet collision and consequently droplet coalescence or agglomerated particles formation are often associated with ultrasonic spray pyrolysis, since reducing droplet size significantly increases the probability for collision[2]. Agglomerated particles are undesirable especially for afterwards sintering purposes, causing hard agglomerates formation and inducing local grain growth and inhomogeneity.

On the contrary of the reports on the mechanisms of particle formation from inorganic salts, solid particles are often generated from metal alkoxides or organic solutions if they undergo polymerization process[29, 33, 42-43]. Another feature that strongly alters the particle morphology is transferring ions into gas phase in the case of volatile precursors[44]. In this case the particles are formed both from gas as well as liquid (solid) phase, leading to the broad size of particle distribution and to the differences in particle morphology. From the viewpoint of difficulties for the stoichiometry retention in the case of multicomponent systems, this feature has to be controlled carefully.

Depending on the process parameters – temperature and residence time, either amorphous or crystalline particles can be obtained. It was shown that proper adjusting of the mentioned parameters enables synthesis of either nanophase, polycrystalline or single-crystal particles by controlling over the mechanisms of grain growth and sintering[2, 28]. Numerous materials, either in the form of thin films or nanostructured/nanoscaled particles as metal oxides, mixed metal oxides, nonoxides and metals have been obtained by this method and have reviewed in literature[2,3,6,13,45,46,47]. The potentials of the aerosol routes for making solid-states structures at the nano size level are virtually unlimited, providing possibilities for new and unique applications in electronics, optoelectronics, catalysis, energy conversion systems, drug delivery etc. It has been reported synthesis of electrode material for solid oxide fuel cells[48, 49], phosphors[47,50], metal-ceramic and ceramic-ceramic nanocomposite particles synthesized in environmental conditions[51, 52] and under microgravity[53]. The examples of experimental set-up for the spray pyrolysis developed at the several research centers and universities are presented at **Fig. 5**.

The program of controlled and sophisticated powders and films synthesis has been realized in the Institute of Technical Sciences of the Serbian Academy of Sciences and Arts (ITS SASA) since past two decades. In the framework of this research, the method of aerosol synthesis of nanophased powders
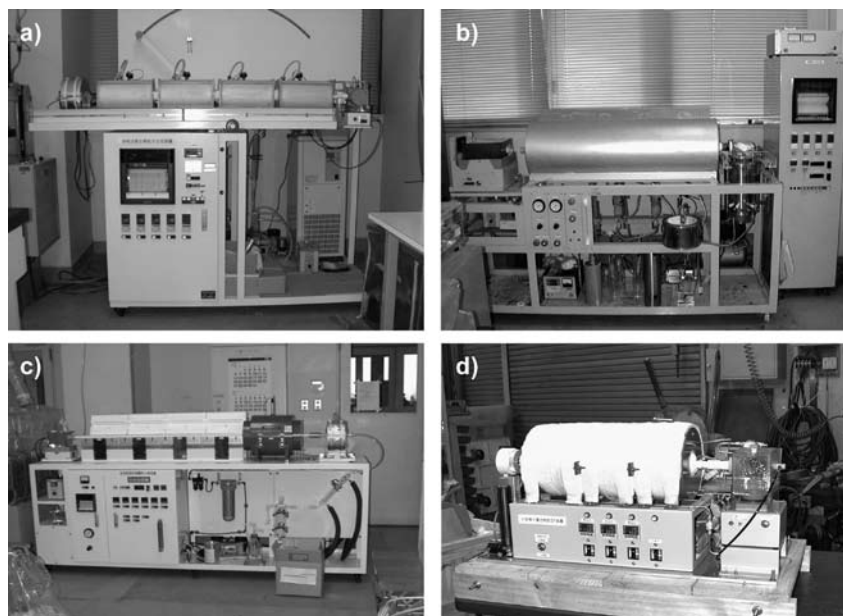
Fig. 5. Experimental set-up in Japan Fine Ceramic Centre, Nagoya (a,b,c), with 4 heating zones, $T_{max}=1000℃$ [48-50]; 4 separating heating zones, $T_{max}=1000℃$ for the synthesis of ceramic-metal nanocomposites; 5 heating zones, $T_{max}=1200℃$ for the synthesis of ceramic-ceramic nanocomposites[51, 52], respectively; Osaka University, JWRI (d) for the synthesis of ceramic nanoparticles under microgravity[53] (with courtesy of Dr. Ohara, Osaka University, JWRI, Japan).

and films is developed together with the experimental and pilot set-up [**Fig. 6**]: the experimental set-up is based both on electrospray (TDI) and ultrasonic (800kHz, 1.3,1.7 and 2.5 MHz, RBI) atomizing systems, while a pilot plant is based on twin-fluid atomization technique, equipped with a Scanning Mobility Particle Sizer (TDI) for in-situ determination of aerosol properties. It offers the opportunity for the synthesis of both monodisperse and polydisperse nanoscaled particles in different oxide and nonoxide systems. Moreover, a Pyrosol technique for thin film synthesis through aerosols is developed, too. Based on these techniques, the synthesis of fine, spherical, submicronic powders either in crystal or amorphous state based on oxides, metals and non-oxides have been processed as follows: ZnO[38,41,54,55], ZnO-Pt(IV)[56], ZnO- Ru(III)[57],, $BaTiO_3$[42], ZnO-Cr_2O_3 spinel[34], Al_2O_3 based materials[58,59], Ni, NiO[60], SiC[61], Q-TiO_2[62], nano-composites Ag:(Bi,Pb)-2223[15,63,64], phosphors, Gd_2O_3:Eu[10,65,66,67], Y_2O_3:Eu, $(GdY)_2O_3$:Eu[20,68,69], $Y_3Al_5O_{12}$:Ce[10,70-74], $LiFePO_4$ [75]. Those materials are applicable for electronics, optoelectronics, engineering ceramics, catalysts, biomaterials etc.

3. Opportunities of Hot Wall Aerosol Route (Spray Pyrolysis) for Phoshor Materials Processing

The opportunities for the synthesis of spherical, nonaglomerated particles with uniformly distributed components and phases are of special importance when phosphor materials having luminescence properties are considered. Phosphors represent inorganic crystal structures capable of emitting definite quantities of radiation within visible and/or ultraviolet spectrum as a result of excitation by an external energy source such as electron or a photon beam[76,77,78]. Such properties of these materials are an outcome from the atomic state interactions that occur between luminescent centers and the host lattice material after the excitation. Rare earth ions ($Eu^{2+, 3+}$, Ce^{3+}, Tm^{3+}, Tb^{3+}, Nd^{3+}) and transition metal ions (Cr^{3+}, Mn^{2+}) are commonly used as luminescent centers[79,80]. Luminescent materials are normally utilized in cathode ray tubes for television screens and due to excellent characteristics of these materials their use has increased in the past years due to their application in modern emissive display industry such as flat screens, plasma and electroluminescence screens, etc. The most important properties that luminescent materials should pos-
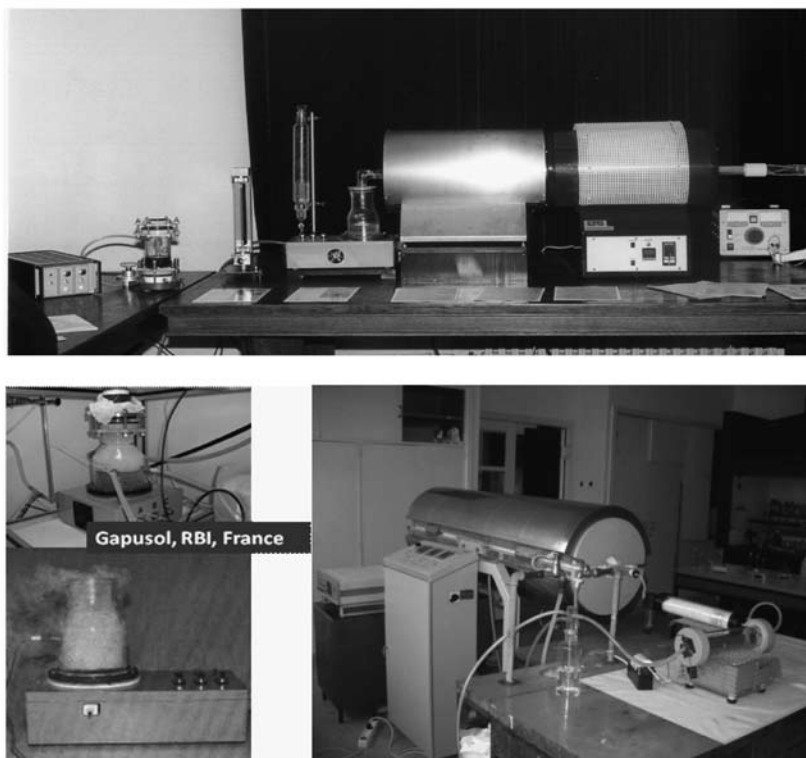

Fig. 6 Experimental set-up at ITS SASA having two (upper) and three (down) heating zones, equipped with an electrostatic precipitator for powder collecting and ultrasonic atomizers, 800 kHz, 2.1 MHz, RBI, Meylan, France (down).

sess are their brightness, spectral energy distribution and decay time[81]. Since luminescence properties are strongly affected by the phosphor crystallinity, phase purity, distribution of activator, surface area and particle morphology[82-84], more efforts have been done in promoting the researches toward new methods for nanoparticles synthesis. Spray pyrolysis method has been recognized as a successful to obtain phosphor powders with high purity, homogeneous distributions of activator centers, narrow distribution of particle size and spherical morphology in nanometric scale [47].

3.1. Gd₂O₃:Eu³⁺

Gadolinia doped with europium has been used in several applications for display devices as effective red phosphor material having improved stability in high vacuum and the absence of corrosive gas emissions under electron bombardment[85]. Since the luminescent behavior is greatly affected by the phosphor particle morphology and compositional homogeneity, the advantages of spray pyrolysis over conventional solid-state synthesis are huge, as already reported in literature[47,82,85, 86].

As part of a programme to develop high grade phosphor particles, spherical in shape, agglomerated-free and with a narrow size distribution, efforts have been made to prepare material using a hot wall spray pyrolysis approach[10, 50, 65]. With regards to that, nano-structured, spherical $Gd_2O_3:Eu^{3+}$ phosphor particles sizing bellow 800nm were synthesized from ultrasonically generated common nitrates solutions (**Fig.7**). As seen, the particle inner structure clearly resolved by the low and high magnification TEM implies the typical particle morphology obtained by spray pyrolysis composed of nano sized primary particles assembled in a spherical secondary particle. Visual inspection of the particle morphology is done by means of STEM nanotomography corresponding to the particle annealed at low temperature (900ºC/12h), as shown in **Fig. 8**[86]. The contrast obtained with HAADF-STEM implies bright and dark areas in a spherical shaped particle sized approx 500nm where dark contrast observed in the tilt series indicates the presence of voids and a rough particle surfaces. In the reconstructed images (**Fig. 8**, right), the better contrast than the original image allows confirming the porous and rough surfaces. It was supposed that the particle roughness is presumably a consequence of the primary particles crystallization, aggregation and growth in the secondary particles caused by the temperature increase.

In comparison to the particle morphology of conventionally obtained phosphor materials, here spherical particle morphology enables high packing
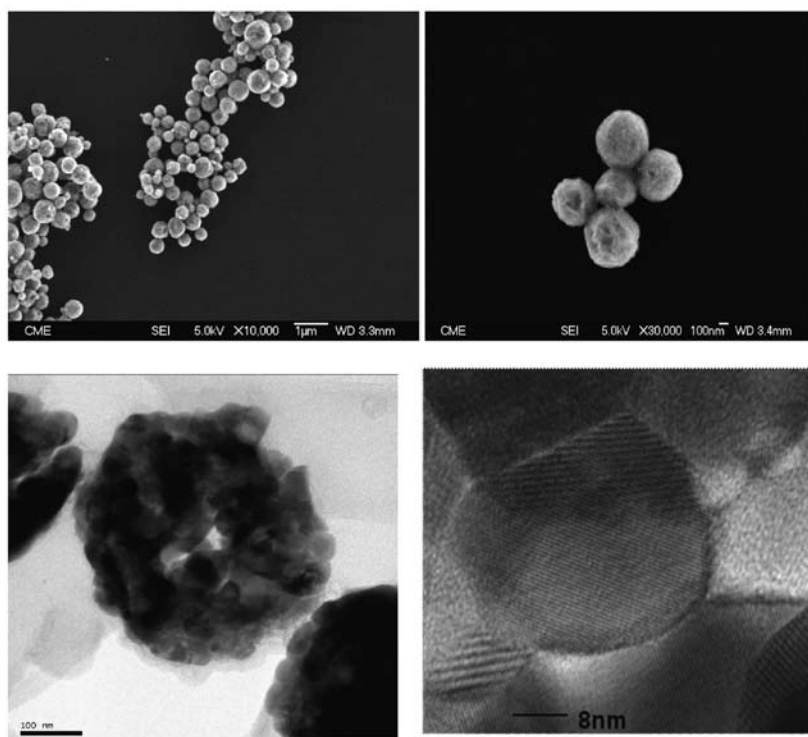
Fig. 7 Field emission scanning electron microscopy (FE-SEM) (upper), TEM, HR-TEM (400 KV JEOL JEM 4000 EX) of the as-prepared Gd₂O₃:Eu particles (down), respectively.
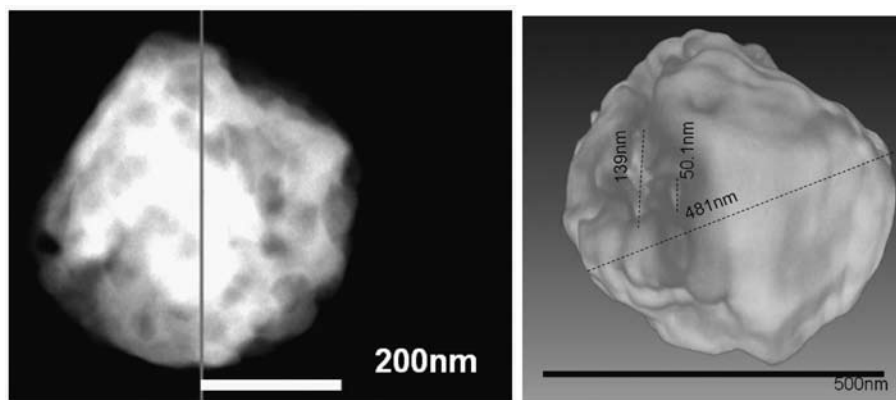
Fig. 8 STEM image of the tomographic tilt series. The vertical line indicates the rotation axis. A Tecnai TEM G² F20 X-TWIN with Fischione "*single tilt*" stage in HAADF mode operated at 200KV TEM was employed (left); reconstructed tomographic image: the inspect 3d v 2.5 X press Edition software and AMIRA software in cross correlation mode was employed (right).

densities, higher brightness and resolution[82]. On the other side, hollow and porous particles have lower signal intensity in comparison with dense spherical particles[86]. Besides, particle roughness and the agglomeration state are very important factors that affect the luminescence signal, implying the necessity to follow the morphology features and correlate them with the process parameters, like temperature, residence time, precursor decomposition behavior etc. In addition, the sensitization of the as-prepared particles is a critical stage in phosphor preparation and sensitivity improves with increasing the crystallinity and homogenization of the Eu dopants within the particles. Success in this processing have been obtained with additional thermal treatments of the as-prepared particles above 800 ℃, where the thermally induced interparticle sintering did not occur and initially obtained morphological features were preserved[65].

Detailed phase and structural analysis proceeded in accordance to XRPD, TEM-HRTEM and EFTEM analysing methods, proved uniform compositional distribution of the constitutive elements along the particles obtained *via* spray pyrolysis as seen from the corresponding gadolinium and europium EFTEM spectra (**Fig.9**). EFTEM-EELS spectrum obtained for Gd_2O_3:Eu^{3+} particles additionally annealed at 900ºC/12h (gray line) and 1000℃ /12h (black line) in the ELNES region show the Gd M4 and Gd M5 signal for both samples (around 1185ev-1187ev) and the Eu *M5* and Eu *M4* signal around 1131ev-1186ev. The comparison between the spectrum indicates the incorporation of the Eu in the Gd matrix, while no changes in the energy and intensity *M4/M5* ratio (0.83) indicates a (+3) oxidation state in the samples with different Eu content and thermal treatment (**Fig. 10**).

Host gadolinium oxide exhibits two polymorphic forms, low temperature (cubic) and high temperature (monoclinic), so several studies dealing with the investigation of Gd_2O_3 crystal phases development dur-
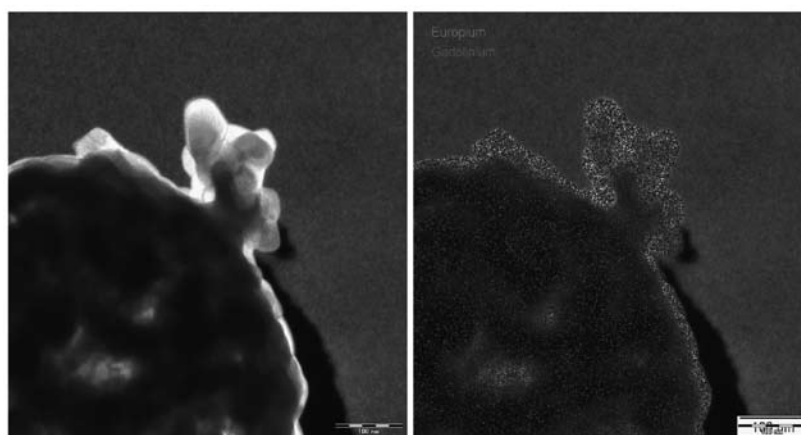
Fig. 9 The low magnification EFTEM images, Libra, 120kV, with a corrected 90° OMEGA energy filter.
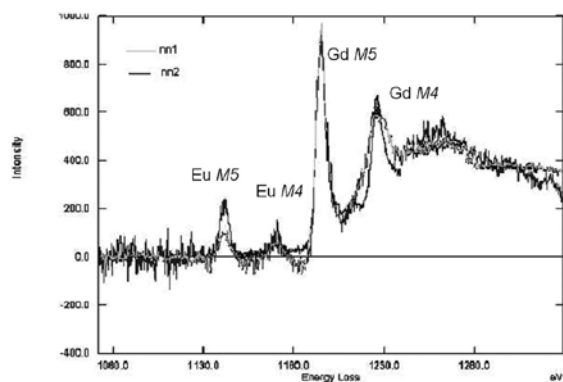
Fig. 10 EFTEM-EELS spectrum obtained for Gd_2O_3:Eu particles treated at 900℃/12h (gray line) and 1000℃/12h (black line) in the ELNES region. A 120 KV LIBRA transmission electron microscope with omega filter in column and EELS spectrum (three windows method) was used.

ing aerosol synthesis and their relationship with luminescence properties were reported[10,82,87,89]. XRPD revealed here the presence of two crystalline cubic phases in as-prepared powders: a bcc phase with *Ia3* space group (a ≈ 10.829(3) Å); and a fcc phase with *Fm-3m* space group (a ≈ 5.6242(1) Å) for the Eu^{3+} less doping concentration[50]. After thermal treatment only the cubic *Ia3* phase has been observed, with the cell parameters affected with Eu^{3+} doping concentration, followed with progressive increase in crystallite size. HR-TEM implied the primary nano particles of the as-prepared powders are associated with the defect structure (**Fig. 7**). After annealing above 900℃, it is evident the better order related to the orientation in the atomic frames and a decreasing of defects content. In confirmation of the stated above, a HRTEM image of the cubic phase with *Ia3* symmetry taken along the〔100〕zone axis is presented at **Fig. 11** indicating high crystallinity and clearly resolved the (002) and (020) atomic planes. In addition, HRTEM

analysis also proved the locally appearance of a monoclinic phase with *C2/m* symmetry taken along the〔1-10〕zone axis. The atomic distance (110) is resolved in the image (**Fig. 11**, right). The appearance of the higher density metastable monoclinic structure is probably a consequence of the extreme synthesis conditions during spray pyrolysis, i.e. high heating rates and short residence time and attributable to the Gibbs-Thomson effect, associated with increased surface tension with nanostructuring[65], (**Fig. 11**).

Luminescence studies carried out in Gd_2O_3:Eu^{3+} phosphor system have demonstrated that annealing and crystalline phases control both the thermoluminescence and radioluminescence signals[65]. Characteristic bands in the emission spectra are assigned to Eu^{3+} ion radiative $^5D_0 \rightarrow ^7F_i$ (i=0,1,2,3,4) transitions. In all the samples maximum intensity peak is at 611 nm wavelength belonging to $^5D_0 \rightarrow ^7F_2$ transition[10,50]. All observed transitions are due to the Eu^{3+} in C_2 crystallographic site except one line, at 581 nm (attributed to $^5D_0 \rightarrow ^7F_1$ transition) that belongs to Eu^{3+} in S_6 crystallographic site.

3.2. Y_2O_3:Eu^{3+}

Y_2O_3 doped with europium is a well known red phosphor material employed in modern high-resolution display devices such as plasma display panels (PDP) and field emission displays (FED)[47]. The incorporation of gadolinium in the yttria matrix may significantly contribute to the luminescent properties and x-ray absorption coefficient thus increasing the field of application in optoelectronic devices such as ceramic scintillators for computed tomography.

The interest of the Y_2O_3 has been broadly known due to its particularly relevant physical and functional properties, including the crystallographic stability, a
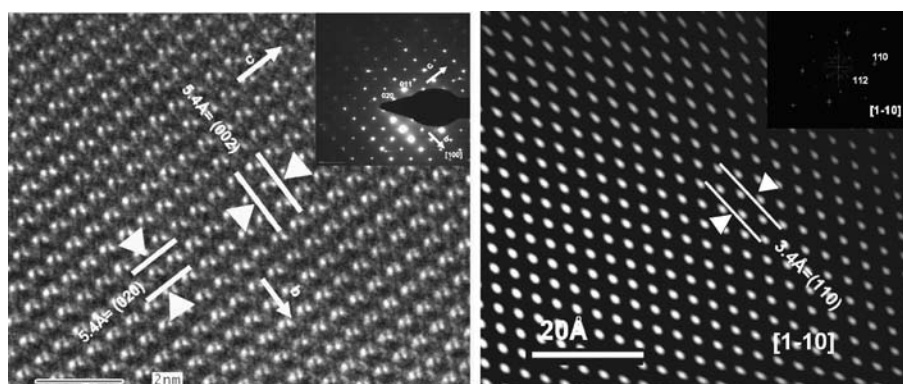
Fig. 11 HRTEM images of the cubic *Ia3* phase with the corresponding indexed electron diffraction pattern (left) and monoclinic *c2/m* phase with the fft indexed along the [1-10] (right) taken by Titan 80-300™ TEM, 300KV and Tecnai F 20 TEM, 200 KV, respectively.

wide band energy gap (5.5e.v.) and the ability to be a host material for rare earth ions. Yttrium oxide is a good phosphor material with different luminescent spectra depending on the luminescent center by which it is activated (for example Eu, Tb, Dy, Tm or Nd); doped with Eu^{3+} is a well known red phosphor in flat panel displays[90-92]. In particular, it has been shown that if in nanostructure form it possesses improved quantum efficiency while the mixed oxide with rare earth ions (RE), the $RE_xY_{2-x}O_3$ type, represents a new group of superconducting materials[93]. Yttria represents one of the best host materials for rare earth ions due to the fact that its ionic radii and crystal structure are very similar to the ionic radii and crystal structure of the rare earth ions[82]. There are several crystal structures of Y_2O_3: cubic, type Mn_2O_3, which represents a stable equilibrium structure under stationary conditions and monoclinic structure with space group *C2/m* that can be formed under extreme synthesis conditions[65,94].

The nanostructured particles of Y_2O_3 doped with Eu^{3+} were processed through the spray pyrolysis method from nitrate precursors[20]. Synthesis was carried out with an ultrasonic aerosol device operating at 1.3 MHz in air atmosphere connected with a triple-zone tubular flow reactor (200-700-900℃) (**Fig. 6**). Particles were submitted to post-thermal treatments at temperatures among 1000 and 1200℃ for 12hours in order to increase the crystallinity and uniform distribution of doped centers. The particles obtained were spherical, having narrow size distributions, high compositional homogeneity and were in un-agglomerated state (**Fig. 12**). Exceptionally, sintering start point was noticed in the case of the samples thermally treated at 1200℃. That is, TEM analysis revealed neck formation between secondary spherical particles[10, 69].

The *Ia3* phase has been identified by XRD and TEM-HRTEM/FFT in both as-prepared and thermally treated samples. No intermediate phase is observed along the particles. Rietveld refinement revealed that crystallite size of the as-prepared powders was around 20nm while sufficient energy supply during the thermal treatment led to crystallite growth (40-130nm for annealing temperatures 1000-1200℃, respectively) and affected structural relaxation (lower values of microstrain in comparison to the values for ap samples) (**Table2**).

Functional characterization done through the determination of photoluminescent characteristics showed typical emission spectra of Eu^{3+} ion incorporated into yttrium oxide. Emission spectra were obtained at room temperature through excitation of Eu^{3+} ion into $^5L_6$ energy level under 393nm wavelength (**Fig. 13**). The emission lines of Eu^{3+} were ascribed to $^5D_0 \rightarrow {}^7F_j$ (j=1, 2, 3, 4) spin forbidden *f-f* transitions and the main emission peak corresponded to clear red emission at 611nm. Detailed analysis of the emission spectra showed that they consist out of sharp peaks, originating from Eu^{3+} ion incorporated into C_2 site, while only one week line belonging to Eu^{3+} ion incorporated into S_6 site was observed. Maximum Stark splitting (ΔE) of the $^7F_1$ manifold, occurring under the influence of the crystal field, was in agreement with theoretical values Y_2O_3:Eu^{3+} ($\Delta E(Y_2O_3) = 355cm^{-1}$)[95].

Based on the fluorescence decay curves of the $^5D_0$ emitting level it was concluded that applied synthesis method (spray pyrolysis) leads to the formation of nanostructured powders having longer lifetimes in comparison to Y_2O_3:Eu^{3+} in its bulk form (τ ($^5D_0 \rightarrow {}^7F_2$)$_{theor}$=1.0ms ($Y_2O_3$))[96]. Also, it was shown that samples with doping concentration of 10 at% Eu^{3+} had lower $^5D_0$ lifetimes (around 1.2 ms) in comparison to 5 at% (around 1.4 ms) leading to a conclusion that in the case of higher doping level concentration quenching occurs (**Table 2**).

Through the analysis of lifetime values for Eu^{3+} $^5D^1$ emitting level for Y_2O_3 with 5at% of Eu^{3+} the influence of thermal treatment was monitored (**Fig. 13**).
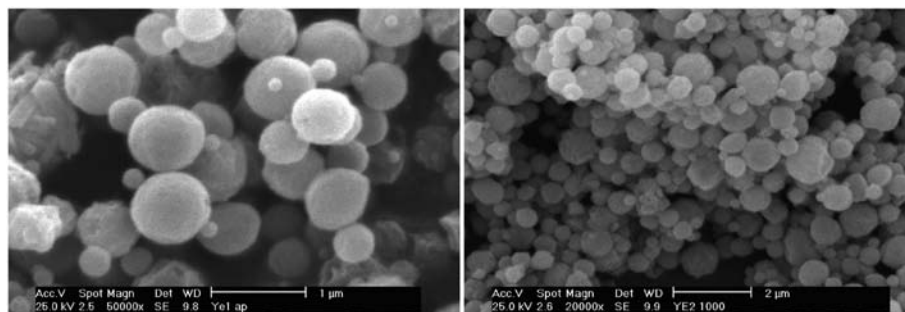
Fig. 12 $(Y_{0.95}Eu_{0.05})_2O_3$ (left) and $(Y_{0.90}Eu_{0.10})_2O_3$ (right) thermally treated at 900℃ and 1000℃, respectively.

Table 2 Main structural parameters derived through Rietveld refinement and characteristics of the luminescent measurements for Y_2O_3:Eu^{3+} system[20]

|	Y_2O_3:Eu^{3+} yeₐB A-doping concentration Eu^{3+}(at%) B- annealing temperature(℃); ap- as-prepared sample							
	ye5 ap	ye5 1000	ye5 1100	ye5 1200	ye10 ap	ye10 1000	ye10 1100	ye10 1200
cs (nm)	19.14	40.55	60.06	129.53	20.11	40.94	66.99	132.89
a (Å)	10.620	10.616	10.616	10.616	10.632	10.628	10.623	10.628
ms (%)	0.432	0.189	0.0607	0.0963	0.529	0.197	0.0794	0.0402
$^5D_0 \rightarrow {}^7F_0$ (C2) (nm)	580.3	580.4	580.4	580.4	580.4	580.4	580.4	580.4
$^5D_0 \rightarrow {}^7F_1$ (S6) (nm)	582.1	582.3	582.2	582.2	582.2	582.0	582.1	582.1
$^5D_0 \rightarrow {}^7F_1$ (C2) (nm)	587.1	587.2	587.1	587.2	587.1	587.2	587.2	587.2
	592.9	592.8	592.8	592.9	592.8	592.8	592.8	592.8
	599.2	599.1	599.2	599.4	599.2	599.2	599.2	599.2
ΔE (cm^{-1})	344.0	338.2	344.0	346.5	344	341	341	341
τ ($^5D_0 \rightarrow {}^7F_2$) (ms)	1.47	1.46	1.40	1.42	1.24	1.21	1.14	1.14
τ_{avr}($^5D_1 \rightarrow {}^7F_2$) ($\mu$s)	11.33	18.97	19.74	19.78	/	/	/	/
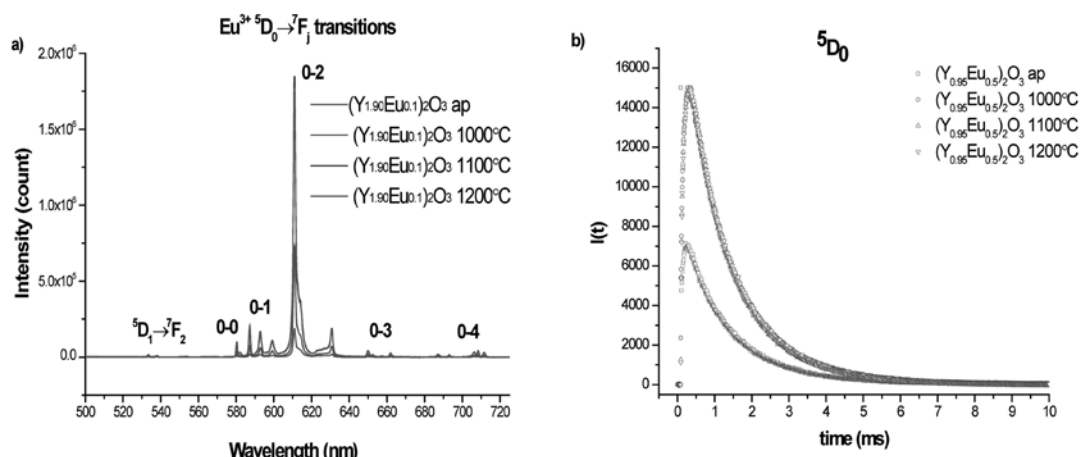
Fig. 13 Emission spectra of $(Y_{0.90}Eu_{0.10})_2O_3$ system (left) and lifetime values of $(Y_{0.95}Eu_{0.05})_2O_3$ system under λ_{ex}=393nm (λ_{em}=611nm) (right)[20].

Namely, as-prepared powders had a lower value of these parameter (around 11 μs) while the value for thermally treated was slightly higher (around 20 μs). Knowing that decrease of emission intensity from $^5D_1$ emitting level is due to increased probability of cross-relaxation mechanism which occurs when there is an increase of Eu^{3+} concentration in the yttria host lattice[97] it was concluded that cross-relaxation effect was stronger in the case of as-prepared samples. Above stated observations indirectly depicted more homogeneous distribution of Eu^{3+} ions in case of the annealed samples. [68,98,99].

3.3. $(Y,Gd)_2O_3$:Eu^{3+}

$(Y_{1-x}Gd_x)_2O_3$:Eu^{3+} system, where the gadolinium content was varied ($\times$=0.25, 0.50, 0.75), has been synthesized throughout the same conditions as Y_2O_3:Eu^{3+}. TEM investigations revealed that these systems poses the same morphological features as yttrium oxide system i.e. particles possess spherical filled morphology. Additionally SAED patterns revealed polycrystalline nature of the particles, while the ring width implied high defect content in as-prepared samples **Fig. 14**. Through XRD and TEM/SAED analysis it was also shown that gadolinium content had influence on the structural phase characteristics. To be exact, as-prepared samples with composition $\times$=0.25, 0.50 had solely *Ia3* phase, but the sample compositionally closest to pure Gd_2O_3, with $\times$=0.75, showed the same characteristics as gadolinium oxide synthesized under similar conditions. Apart from primary, cubic bcc *Ia3* phase a second cubic fcc
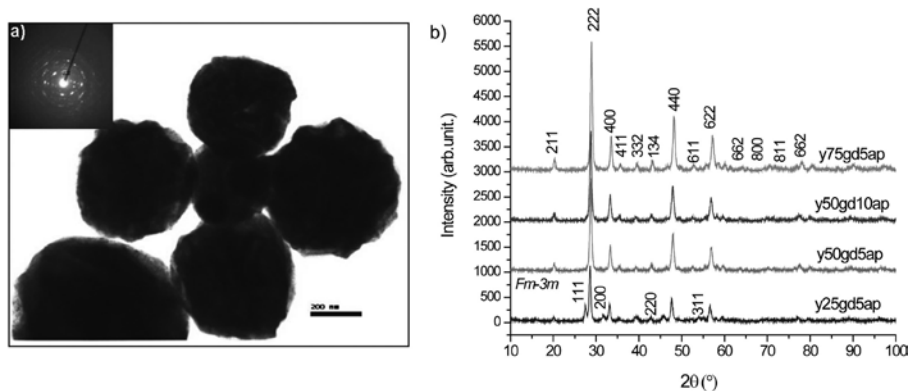
Fig. 14 TEM/SAED image for as-prepared $(Y_{0.50}Gd_{0.50})_2O_3:Eu^{3+}$ powder with 10at% of Eu^{3+} (left) and XRD diffraction patterns of the as-prepared samples for $(Y_{1-x}Gd_x)_2O_3:Eu^{3+}$ system indentifying *Ia3* phase as a primary phase in all the samples and for the sample x=0.25 peaks belonging to *Fm-3m* are denoted (right).

phase with *Fm-3m* space group was confirmed in ap samples[20,69]. All the as-prepared samples where thermally treated at 1100℃ for 12h and in this case only *Ia3* phase prevailed.

Observing the optical properties, the same characteristic emission spectra of Eu^{3+} ion were seen as in the case of pure $Y_2O_3:Eu^{3+}$ system. Detailed analysis of the emission spectra showed that in the case of $(Y_{1-x}Gd_x)_2O_3:Eu^{3+}$ system a linear increase of maximum Stark splitting (ΔE) occurs with the increase of gadolinium content (**Table 3**), i.e. with the increase of lattice parameters. Since maximum splitting of the $^7F_1$ manifold is affected by crystal field strength parameter in a proportional way, the increase of ΔE value with the increase of gadolinium content could be treated as a clear indication of almost perfect mixing in solid solutions of $(Y,Gd)_2O_3:Eu^{3+}$ system[20,98].

When doped with 5at% mixed $(Y_{1-x}Gd_x)_2O_3:Eu^{3+}$ oxides, thermally treated at 1100℃, had similar lifetime values of $^5D_0$ emitting level in comparison to yttria with same doping concentration (around $1.4 \mu s$). In the case of ×=0.50, doping was done with 5 and with 10at% of Eu^{3+} and in these case $^5D_0$ lifetime of the sample with higher doping concentration was significantly smaller i.e. $0.86 \mu s$. It indicated concentration quenching and that $(Y_{1-x}Gd_x)_2O_3:Eu^{3+}$ with ×=0.50 and 10 at% of Eu^{3+} had inferior properties than the material in bulk form. Relatively high values of $^5D_1$ lifetimes for thermaly treated $(Y_{1-x}Gd_x)_2O_3:Eu^{3+}$ powders with 5at% revealed, as in the case of $Y_2O_3:Eu^{3+}$, implied homogeneous distribution of the doping ion.

3.4. $Y_3Al_5O_{12}$ (YAG): Ce^{3+}

The $Y_3Al_5O_{12}$ (YAG) is optically isotropic mate-

Table 3 Main structural characteristics derived through Rietveld refinement and characteristics of the luminescent measurements for $(Y_{1-x}Gd_x)_2O_3:Eu^{3+}$ system annealed at 1100℃ [20]

	$(Y_{1-x}Gd_x)_2O_3:Eu^{3+}$ y_A gdBT A- yttrium content; B-doping concentration of Eu^{3+}(at%); T-annealing temperature			
	$y_{75}gd_5$ 1100	$y_{50}gd_5$ 1100	$y_{25}gd_5$ 1100	$y_{50}gd_{10}$ 1100
cs (nm)	155.94	202.63	55.25	191.36
a (Å)	10.667	10.724	10.771	10.730
ms (%)	0.0329	0.0563	0.0333	0.0195
$^5D_0 \rightarrow {}^7F_0$ (C$_2$), nm	579.9	580.0	580.0	579.9
$^5D_0 \rightarrow {}^7F_1$ (S$_6$), nm	581.6	581.6	581.4	581.4
$^5D_0 \rightarrow {}^7F_1$ (C$_2$), nm	586.8	586.9	587.1	586.9
	592.3	592.3	592.2	592.2
	598.5	598.3	598.2	598.4
ΔE (cm^{-1})	333.2	324.7	316.1	327.5
τ ($^5D_0 \rightarrow {}^7F_2$) (ms)	1.36	1.25	1.32	0.86
$\tau_{avr}(^5D_1 \rightarrow {}^7F_2)$ (μs)	14.3	13.9	13.6	/

rial with high thermal conductivity. Doped with rare earth ions it represents very useful phosphor material for variety of display applications including cathode ray tube, low voltage field emission display, and backlight source. Specially cerium doped YAG (YAG: Ce^{3+}), as a yellow-emitting component for the production of a white light, is a comprehensively studied previous years due to urgent demand for alternative light source in an illumination and display area. The broad Ce^{3+} emission band originates from the 4f-5d electronic transition with intensive side bands due to vibronic coupling to the lattice and local vibration modes in the YAG lattice. Due to this YAG:Ce^{3+} easily convert blue emission from blue light emitting diode (LED) into white LED. Even a lack of cerium emission toward the red region can be suppressed by a co-doping (Tb^{3+}) or cation substituting (Ga^{3+} or Gd^{3+}) making presently this material to be the phosphor of choice in commercial white LEDs[100].

First publication related to luminescence investigation in YAG:Ce^{3+} system dated from 1967[101]. Compared with this traditionally produced garnet by solid-state reaction between the component oxides, today's phosphor materials usually produced through soft-chemistry processes posses many advantages thanks to their certain structural and morphological characteristics. The field of aerosol processing was intensively developed in the last 10 years and many phosphorous materials have been produced up to now[47]. Processing of YAG:Ce^{3+} powder *via* spray pyrolysis (ultrasonic and FEAG) has been previously reported[102,103]. Significant advance is shown due to the mixing of starting reactants at molecular scale, but obtaining of the pure garnet phase was hindered by retaining of amorphous phase in synthesized powders. Therefore, annealing process at high temperatures was applied for the crystallization and activation of cerium-doped YAG particles. In latter work[104], it was shown that the PL intensity of YAG:Ce^{3+} particles was strongly affected by doping concentration of cerium, annealing temperature, mean particle size, and particle morphology. The non-aggregated spherical particles of YAG:Ce^{3+} (1at%) annealed at 1300℃ showed the maximum photoluminescence emission. Several papers devoted to the same topic were reported in the following years, highlighting the complexity of synthesis - structure relation towards achieving optimized phosphors properties. It was shown that concentration of nitrates solution and the flow rate of nitrogen used as a carrier gas have the major impact on the productivity of the spray pyrolysed particles[104]. Significant mor-

phological and functional enhancement through BaF_2 flux introduction in common nitrates solution during spray pyrolysis resulted in the intensification of the maximum peak intensity of the prepared YAG:Ce^{3+} phosphor powders in comparison to that of the commercial phosphor powders[105]. The addition of urea into nitrate precursor contributes to nanoparticles formation due to its combustion in the flame zone and improves their optical performance[106]. Further enhancing of the YAG:Ce^{3+} luminescence efficiency can be realized through Tb^{3+} co-doping due to occurring of the effective energy transfer from Tb^{3+} to Ce^{3+} in YAG host lattice[107]. But in all of above reports insitu generation of garnet phase during spray pyrolysis is omitted or associated with $Y_4Al_2O_9$, (YAM) or $YAlO_3$ (YAP) phases appearing so additional thermal treatment of processed powder is obligatory. The technique of spray pyrolysis was employed also to produce homogeneous solid solutions in the Al_2O_3–Y_2O_3 system at temperatures as low as 150-300℃, owing to the prevention of segregation of the precursors prior to YAG phase crystalization[108]. Another attempt has been made using "single-source" precursors (alkoxides and glycolates) instead of "multiple-source" precursor[109]. The lack of formation of YAG in all the spray pyrolysis experiments was ascribed to the short heating times and fast heating rates, which resulted in the formation of kinetic products.

Rationalization of the sequence for nanocrystalline YAG:Ce^{+3} phase evolution in the particles synthesized by ultrasonic spray pyrolysis method through variation of processing parameters or precursors composition was also the topic of our research [10,70-74]. It was shown that particle morphological and structural characteristics are dependent on the applied synthesis methodology, especially regarding the precursors solution modification. Synthesis from common nitrates precursors was performed at 900℃ in a tubular flow reactor using the air to carry the aerosol. Short residence time during synthesis resulted in multiphase powder generation. Beside garnet phase, YAM and Y_2O_3 were also detected[71]. Synthesized particles were submicronic in size, highly spherical and unagglomerated (**Fig. 15**). They exhibit rough surface implying that are built from primary nanoparticles[70]. Their general morphology did not change significantly with annealing, but their roughness increase further due promoted crystallization affecting their specific surface[72]. Incorporation of Ce^{3+} ions at the host is confirmed with the broad emission having peak maximum at 533nm[70]. The interpretation of the thermo- and radio- luminescence signals from
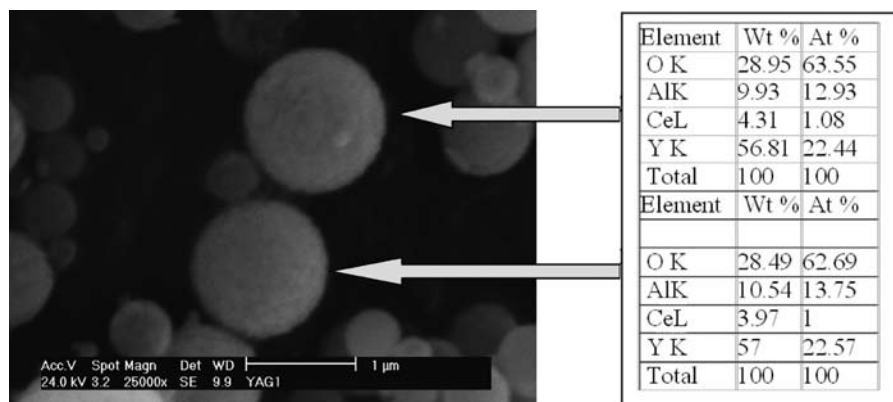
Element	Wt %	At %
O K	28.95	63.55
Al K	9.93	12.93
Ce L	4.31	1.08
Y K	56.81	22.44
Total	100	100

Element	Wt %	At %
O K	28.49	62.69
Al K	10.54	13.75
Ce L	3.97	1
Y K	57	22.57
Total	100	100

Fig. 15. SEM of the YAG:Ce^{3+} particles obtained through spray pyrolysis of nitrate solution at 900℃ and annealed at 1000℃ (6h); corresponding EDS analysis.

the YAG:Ce^{3+} powders implies that the cerium ions are not readily accommodated on the YAG lattice sites during synthesis[65]. Even after annealing cerium ions do not offer a favourable excitation decay path; instead, there are broad emission bands typical of the host lattice defect sites and a very weak luminescence via the cerium on pathway near 300nm. The complexity of the temperature dependence of the TL as a function of wavelength also suggests that a variety of independent defect sites contributes to the TL. They also indicated numerous anomalies in the temperature dependence of their luminescence lifetime data.

To investigate the nature of the multiphase powder obtaining, an amorphous material with composition corresponding to yttrium aluminum garnet phase with same content of cerium has been synthesized at 320℃ using a similar spray pyrolysis route. Precursor-derived amorphous phase crystallized at temperatures as high as 900 and 1000℃ gave multi-phased powders with different compositions after 3h of annealing (YAG, YAP, YAM), while prolongation of treatment at higher temperature result in pure YAG phase formation (**Fig. 16**)[73].

In order to achieve additional heating during YAG:

Ce^{3+} synthesis urea-assisted spray pyrolysis was employed[111]. This route can be regarded as a self-combustion synthesis confined within a droplet where urea acts as an *in-situ* source of thermal energy due to its decomposition. The as-prepared non-agglomerated amorphous powder has broad particle size distribution (200-1400nm) (**Fig. 17**). They were additionally thermally treated in air at 1000 and 1100 ℃ for 6h preserving their morphological characteristics. Despite of precursor modification during synthesis, performed annealing did not yield pure YAG:Ce^{3+} product. While lower temperature is favorable for YAP and YAM phase segregation, increase of heating temperature enhanced YAG phase formation with YAM phase retention.

Having this in mind, preservation of the molecular homogeneity during precursor synthesis was done through polymerization with an organic complexing agent EDTA and ethylen glycol (EG)[74]. Two reactions are involved, a complex formation between EDTA and metals (via four carboxylate and two amine groups) and esterification between EDTA and EG. Ultrasonically generated aerosol droplets were decomposed at 600℃ in argon atmosphere. Following the initial attempt in providing pure YAG:
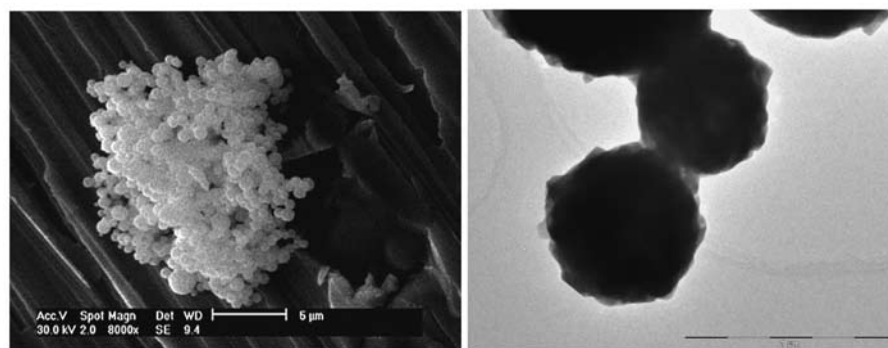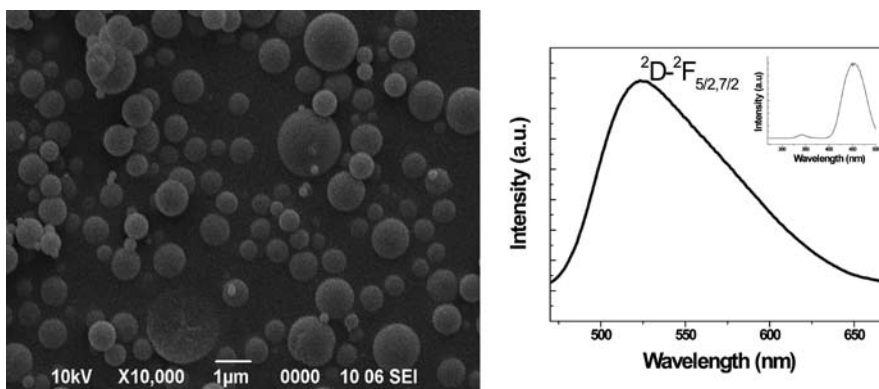

Fig. 16 SEM and TEM of the YAG:Ce^{3+} particles obtained through spray pyrolysis of nitrate solution at 320℃ and annealed at 1000℃ (6h).

Fig. 17 SEM of the as-prepared YAG:Ce^{3+} particles obtained through urea-assisted spray pyrolysis at 900℃; PL spectra of particles treated at 1100℃ (3h).

Ce^{3+} phase generation the particles were additionally thermally treated for 3h in air at 1000℃ and 1100℃. Comprehensive structural analysis implied that garnet phase was formed without contamination of other phase having different aluminum yttrium composition even at the lower annealing temperature and in a much shorter time. The spherical dense particles comprised grained-like structure, since they are composed of nanosized garnet monocrystals (**Fig. 18**). Although uncompleted, cerium incorporation in garnet matrix is confirmed by broad green-yellow emission spectra in the range of 470-670 nm peaking at 521nm. With this optimization of the spray pyrolysis reaction conditions towards synthesis of pure, un-agglomerated YAG:Ce^{3+} particles with spherical shape and filled morphology were achieved.

4. Conclusions

Aerosol route represents a versatile synthesis method for processing novel functional materials. An insight into the diversity of this method and materials that could be produced was given within this paper with the highlight on hot-wall aerosol synthesis of phosphor particles based on Gd$_2$O$_3$:Eu, Y$_2$O$_3$:Eu, (Y$_{1-x}$Gd$_x$)$_2$O$_3$:Eu and Y$_3$Al$_5$O$_{12}$:Ce which are a part of the current research in the Institute of Technical Sciences of SASA, Serbia. As it was summarized, the syntheses from the aerosol are found to be of great value since they result in well defined phosphor powder characteristics essential for achieving higher brightness and resolution in displays. Particularly, it was shown that spray pyrolysis is one of the simplest among them and is capable in ensuring particle spherical morphology, good crystallinity and uniformity in size and shape. Those characteristics enhance uniform distribution of the luminescent centre in the host matrix influencing final luminescence properties.

Targeted cubic crystal structure of RE$_2$O$_3$:Eu oxide powders (RE=Gd,Eu) was obtained in all as-prepared samples and it persisted as the solely phase through-
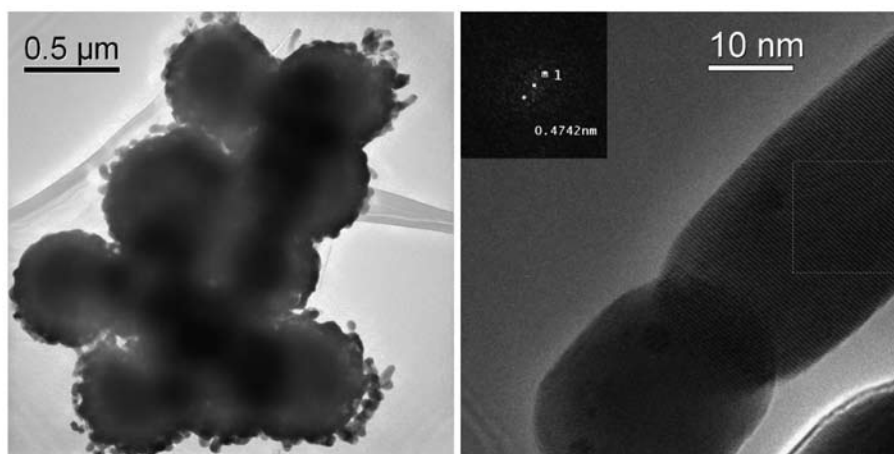
Fig. 18 TEM/HRTEM/FFT of the YAG:Ce^{3+} particles obtained from polymeric precursor solution through spray pyrolysis at 900℃; annealed at 1100℃; FFT inset confirm *Ia-3d* phase formation (211 plane).

out the thermal treatment (1000-1200℃ /12h) which led to the improvement of crystallinity. Appearance of secondary fcc *Fm-3m* phase in as-prepared samples of Gd_2O_3:Eu^{3+} and mixed oxide with highest content of gadolinium $(Y_{0.25}Gd_{0.75})_2O_3$:Eu^{3+} was identified through XRD and TEM/SAED analysis. Additionally, in the case of Gd_2O_3:Eu system HRTEM analysis revealed local appearance of a metastable, monoclinic phase at temperatures above 1100℃ associated with a high content of interfaces and high defect content. Generally, in the case of RE_2O_3:Eu oxides a good control over morphological features was accomplished. Controlled synthesis parameters led to the formation of powders consisted out of spherical, non- agglomerated particles with narrow size distribution (300-800nm). TEM/HRTEM analysis revealed their nanostructural nature (primary particles as low as 20 nm) and filled morphology. Functional characterization of RE_2O_3:Eu revealed typical emission spectra of Eu^{3+} ion incorporated into rare earth oxides with dominant red emission peak at 611nm. The development of local defect structure, depending on the time-temperature history of phosphor processing, may influence the emission spectra causing broader luminescent lines. For $(Y,Gd)_2O_3$:Eu oxides the increase of Gd content in the yttria matrix had an influence on the spectra and it was observed throughout the increase of maximum Stark splitting (ΔE) of the $^7F_1$ manifold. Such behavior was treated as a clear indication of almost perfect mixing in solid solutions of $(Y,Gd)_2O_3$:Eu^{3+} system. Based on the fluorescence decay curves of the $^5D_0$ emitting level of Y_2O_3:Eu^{3+} and $(Y,Gd)_2O_3$:Eu^{3+} systems it was concluded that applied synthesis method led to the formation of nanostructured powders having longer lifetimes in comparison to Y_2O_3:Eu^{3+} in its bulk form. Also, these analyses showed that concentration quenching occurs for the case of 10 at% doping concentration of Eu^{3+} in comparison to 5 at% due to lower values of $^5D_0$ lifetimes.

In the case of YAG:Ce^{3+} the control over their morphological properties was not completely achieved due to the fact that fully dense particles were not generated from nitrate precursors. Additionally, applying the concept of low temperature aerosol decomposition resulted in preservation of the desired powder morphology but formation of YAG phase was still followed by YAM and Y_2O_3 phases. The drawback was in the fact that high heating rates and short residence time, inherent to spray pyrolysis process, led to the formation of kinetically stable phases rather than the thermodynamically stable target YAG phase. Since spray pyrolysis offers different approaches for controlling of the particle morphology and composition, obtaining of the YAG:Ce^{3+} particles with spherical and filled morphology was done through introduction of polymeric precursor solutions. The absence of intermediate phases implied that observed differences in solubility of yttrium and aluminum sources (liable for sequential precipitation and phase segregation) could be prevailed through homogeneous dispersion of Y^{3+} and Al^{3+} ions into polymeric organic network formed by esterification. Enhancement in PL intensity of synthesized particles indicated reduced dimensionality of their primary entities (crystallites) and homogeny distribution of cerium ion in the YAG host lattice.

References

1) Tuller, H. (1997): Solid State Electrochemical Systems-Opportunities for Nanofabricated or Nanostructured Materials, J. Electroceram., 1(3) pp.211-218.

2) Messing, G.L. Zhang S.-C. and Jayanthi, G.V. (1993): Ceramic Powder Synthesis by Spray Pyrolysis, J. Amer. Ceram. Soc., 76 (11) pp.2707-805.

3) Gurav, A. Kodas, T. Pluym T. and Xiong, Y. (1993): Aerosol Processing of Materials, Aerosol Sci. Techn., 19, pp. 411-52.

4) Kodas, T. T. Hampden-Smith, M. J. (1999): Aerosol Processing of Materials, Wiley-VCH .

5) Milosevic, O. (1999): Aerosol Synthesis of Nanostructured Materials" ; in Advanced Science and Technology of Sintering, Edited by B. Stojanovic, M.V.Nikolic and V. Skorokhod, Kluwer Academic/Plenum Publishers, New York, pp.103-111.

6) Madler, L. (2004): Liquid-fed Aerosol Reactors for One-step Synthesis of Nano-structured Particles, KONA Powder and Particle Journal, 22, pp.107-119.

7) Okuyama K. and Lengorro I. W.(2003): Preparation of Nanoparticles via Spray Route, Chem.Eng. Sci., 58, pp.537-547.

8) Gurav, A., Kodas, T., Kauppinen, E., Joutsensaari,

J. and Zilliacus, R. (1994): Phase evolution and gas-phase particle size distributions during spray pyrolysis of (Bi,Pb)-Sr-Ca-Cu-O and Ag-(Bi,Pb)-Sr-Ca-Cu-O powders. Nanostr. Mater., 4 (5), pp.583-589.

9) Fukui, T., Ohara S. Naito, M. and Nogi, K. (2003): Performance and stability of SOFC anode fabricated from NiO/SYZ composite particles, J. Euro. Cer. Soc., 23 (15), pp.2963-2967.

10) Milosevic, O., Mancic, L., Rabanal, M.E., Yang, B and Townsend, P.D. (2005): Structural and Luminescence Properties of $Gd_2O_3:Eu^{3+}$ and $Y_3Al_5O_{12}:Ce^{3+}$ Phosphor Particles Synthesized via Aerosol, J.Electrochem. Soc., 152, pp.G707-713.

11) Pratsinis S.E. and Vemury, S. (1996): Particle formation in gases: a review, Powder Techn. 88, pp.267-273.

12) Zachariah M. R. and Huzarewicz, S. (1991): Aerosol processing of YBaCuO superconductors in a flame reactor, J. Mater. Res., 6(2), pp.264-269.

13) Helble, J. J.(1998): Combustion aerosol synthesis of nanoscale ceramic powders, J.Aerosol Sci., 29 (5-6), pp.721-736.

14) Tani, T., Watanabe N. and Takatori, K. (2003): Emulsion combustion and flame spray synthesis of zinc oxide/silica particles, J.Nanopart.Res., 5(1-2), pp.39-46.

15) Mancic, L., Milosevic, O., Marinkovic, B., de Silva Lopes, M.F. and Rizzo, F. (2000) "The influence of urea on the formation process of Bi-Pb-Sr-Ca-Cu-O superconducting ceramics synthesized by spray pyrolysis method" , Mat. Sci. Eng.: B, Vol 76(2), pp.127-132.

16) Lee, S., Son, T., Yun, J., Kwon, H., Messing, G.L. and Jun, B. (2004): Preparation of $BaTiO_3$ nanoparticles by combustion spray pyrolysis, Mater. Lett., 58, pp.2932-2936.

17) Langlet, M., Joubert, J. C. (1992): The pyrosol process or the pyrolysis of an ultrasonically generated aerosol, in: C.N.R.Rao (Ed.), Chemistry of Advanced Materials, Blackwelll Scientific Publications, Oxford, pp.55-78.

18) Smith, A.(2000): Pyrosol deposition of ZnO and SnO_2 based thin films: the interplay between solution chemistry, growth rate and film morphology, Thin Solid Films, 376, pp.47-55.

19) Tucic, A., Marinkovic, Z.V., Mancic, L., Cilense, M., Milosevic, O. (2003): Pyrosol preparation and structural characterization of SnO_2 thin films, J.Mat.Process.Techn., 143-44, pp.41-45.

20) Marinkovic, K. (2009): Structural, morphological and functional properties of nanostructured rare-earth oxides obtained through aerosol synthesis, Master Science Thesis, Belgrade University.

21) Lang, R. J. (1962): Ultrasonic atomization of liquids, J. Acoust. Soc. Am. 34, pp.6-8.

22) Liu, T. Q., Sakurai, O., Mizutani, N., .Kato, M. (1986): Preparation of spherical fine ZnO particles by the spray pyrolysis method using ultrasonic atomization technique, J. Mat. Sci., 21 pp.3698-3702.

23) Lenggoro, I. W., Okuyama, K., Fernandez de la Mora J., and Tohge, N. (2000): Preparation of ZnS nanoparticles by electrospray pyrolysis, J. Aerosol Sci., 31 (1) pp.121-136.

24) Chang, H-W., Okuyama, K. (2002): Optical properties of dense and porous spheroids consisting of primary silica nanoparticles, Aerosol Sci., 33, pp.1701-1720.

25) Ocaña M. and Matijevic, E. (1990): Preparation of uniform colloidal dispersions by chemical reactions in aerosols—V. Tin(IV) oxide, J.Aerosol Sci., 21(6), pp.811-20.

26) Nukiyama, S., Tanasawa, Y. (1993): An experiment on the atomization of liquid, Transactions of the Japan Society of Mechanical Engineering, 5, pp.136-143.

27) Maric, R., Fukui, T., Ohara, S., Yoshida, H., Nishimura, M., Inagaki T. and Miura, K. (2000): Powder Prepared by Spray Pyrolysis as an Electrode Material for Solid Oxide Fuel Cells, J. Mater. Sci., 35, pp.1-8.

28) Gonzales-Carreno, T., Morales, M.P., M. Gracia M. and Serna, C. J.(1993): Preparation of uniform g-Fe_2O_3 particles with nanometer size by spray pyrolysis", Mater. Lett. 18, pp.151-155.

29) Cho, S-Y. Lee J-H. and Park, S-J. (1993): Preparation of spherical SnO_2 powders by ultrasonic spray pyrolysis, J.Am.Ceram. Soc. 76 (3) pp.10-15.

30) Fukui, T., Ohara S. Naito, M. and Nogi, K. Morphogy and Performance of SOFC Anode Fabricated from NiO/YSZ Composite Perticles, J. Chem. Eng. Jpn., 34 (7), pp.964-966.

31) Chang, Y., Park S.B. and Kang, Y.W (1995): Preparation of high surface area nanophase particles by low pressure spray pyrolysis, Nanostr. Mater. 5, pp.777-791.

32) Li, Q., Sorensen, C.M., Klabunde K.J. and Hadjipanayis, G.C. (1993): Aerosol spray pyrolysis synthesis of magnetic manganese ferrite particles, Aerosol Sci. Techn. 19, pp.453-467.

33) Senzaki, Y., Caruso, J., Hampden-Smith, M.J., Kodas T.T. and Wang, L. M., (1995): Preparation of strontium ferrite particles by spray pyrolysis, J. Amer. Ceram. Soc. 78(11) pp.2973-2976.

34) Marinkovic, Z. V., Mancic, L., Maric, R., Milosevic, O. (2001): Preparation of nanostructured Zn-Cr-O spinel powders by ultrasonic spray pyrolysis, J.Europ.Ceram. Soc., 21 (10-11) pp.2051-2055.

35) Koch W. and Friedlander, S. K. (1990): Particle growth by coalescence and agglomeration, J.Aerosol Sci., 21(1) pp.S73-S76.

36) Okuyama, K., Lenggoro, I.W. (2003): Preparation of nanoparticles via spray route, Chemical Engineering Science, 58, pp.537-547.

37) Pluym, T.C., Powell, Q. H., Gurav, A.S., Ward T.L. and Kodas, T.T. (1993): Solid silver particles production by spray pyrolysis, J.Aerosol Sci. 24 (3) pp.383-392.

38) Marinkovic, Z.V., Mancic, L., Milosevic, O. (2004): Nature of structural changes in nanocrystalline ZnO powders under linear heating conditions, J. Euro. Cer. Soc., 24, pp.1929-1933.

39) Jayanthi, G.V., Zhang S.C. and Messing, G.L. (1993): Modeling of solid particle formation during solution aerosol thermolysis, Aerosol Sci.Techn. 19, 478-490.

40) Xiong Y. and Kodas, T. T. (1993): Droplet evaporation and solute precipitation during spray pyrolysis, J.Aerosol Sci. 24 (7) pp.893-908.

41) Milosevic, O., Gagic, V., Vodnik, J., Mitrovic, A., Karanovic, Lj., Stojanovic, B., Zivkovic, Lj. (1997): Synthesis and deposition of ZnO based particles by aerosol spray pyrolysis, Thin Solid Films, 296, pp.44-48.

42) Milosevic, O., Mirkovic, M., Uskokovic, D. (1996): Characteristics and formation mechanism of BaTiO₃ powders prepared by twin-fluid and ultrasonic spray-pyrolysis method, J.Am. Ceram.Soc., 79 (6) pp.1720-22.

43) Odier, P., Dubois, B., Clinard, C., Stroumbos, H. and Monod, P. (1990): Processing of ceramic powders by the spray pyrolysis method; influence of the precursors, examples of zirconia and YBa₂Cu₃O₇, in: Ceramic Trans - Ceramic Powder Science III, G.L. Messing, S. Hirano, H. Hausner ed., American Ceramic Society, Westerville, OH.

44) Xiong, Y., Lyong S.W. and Kodas, T.T. (1995): Volatile metal oxide evaporation during aerosol decomposition, J.Am.Ceram.Soc. 78 (9) pp.2490-2496.

45) Patil, P.S. (1999): Versatility of chemical spray pyrolysis technique, Mater. Chem. Phys., 59, pp.185-198.

46) Uskokovic D. and Jokanovic, V. (2006): Molecular designing of fine particles using aerosol synthesis, in Advances in Dielectric Materials and Electronic Devices, ed. American Ceramic society, Ceramic Transactions, 174, pp.3-14.

47) Jung, S., Kang, Y.C., Kim, J.H. (2007): Generation of phosphor particles for photoluminescence applications by spray pyrolysis, J.Mater. Sci., 42, pp.9783-9794.

48) Fukui, T., Oobuchi, T., Ikuhara, Y., Ohara, S. and Kodera, K. (1997): Synthesis of (La,Sr)MnO₃-YSZ Composite Particles by Spray Pyrolysis, J.Am.Ceram. Soc., 80, pp.261-263.

49) Fukui, T., Ohara, S. and Mukai, K. (1998): Long-Term Stability of Ni-YSZ Anode with a New Microstructure Prepared from Composite Powder", Electrochem. Solid-State Lett., 1, pp.120-122.

50) Milosevic, O., Maric, R., Ohara, S., Fukui, T. (2001): Aerosol Synthesis of Phosphor Particles Based on Eu Activated Gadolinium Oxide Matrices, Ceramic Transactions, 112, Ceramic Processing Sci. VI, pp.101-106.

51) Fukui, T., Ohara, S., Naito, M. and Nogi, K. (2003): Synthesis of NiO-YSZ Composite Particles for an Electrode of Solid Oxide Fuel Cells by Spray Pyrolysis, Powder Technology, 132, pp.52-56.

52) Matsumoto, M., Kaneko, K., Yasutomi, Y., Ohara, S. and Fukui, T. (2002): Synthesis of TiO₂-Ag Composite Powder by Spray Pyrolysis", J. Ceram. Soc. Japan, 110, pp.60-62.

53) Cribier, J-F., Ohara, S. and Fukui, T. (2003): Preparation of ZnO based Particles in a Microgravity environment", J. Mater. Sci. Lett., 22, pp.37-40.

54) Milosevic, O., Jordovic, B., Uskokovic, D. (1994): Preparation of fine spherical ZnO powders by an ul-trasonic spray pyrolysis method, Materials Letters 19, (3-4) pp.165-170.

55) Milosevic, O, Uskokovic, D.(1993): Synthesis of Ba-TiO₃ and ZnO varistor precursor powders by reaction spray pyrolysis, Mat. Sci. Eng. A 168 (2) pp.249-252.

56) Djinovic, V. M., Mancic, L. T., Bogdanovic, G. A., Vulic, P. J., del Rosario, G., Sabo T.J. and Milosevic, O.B. (2005): Aerosol synthesis of pure and Pt-doped ZnO particles using nitrate and pdda-Pt(IV) complex solutions, J. Mater. Res., 20 (1) pp.102-113.

57) Grguric-Sipka, S., Sabo, T., Mancic L. and Milosevic O. (2004): Aerosol synthesis of ruthenium doped ZnO fine particles, J.Aerosol.Sci., 35, pp.S183-184.

58) Janackovic, Dj., Jokanovic, V., Kostic-Gvozdenovic, Lj., Zivkovic, Lj., Uskokovic, D. (1996): Synthesis, Morphology and Formation Mechanism of Mullite Particles Produced by Ultrasonic Spray Pyrolysis", J.Mater.Res., 11 (7) pp.1706-1716.

59) Martin, M.I., Rabanal, M.E., Gomez, L.S., Torralba, J.M., Milosevic, O. (2008): Microstructural and morphological analysis of nanostructured alumina particles synthesized at low temperature via aerosol route, J.Eur.Cer.Soc., 28, pp.2487-2494.

60) Stopic, S., Ilic, I., Nedeljkovic, J., Rakocevic, Z., Uskokovic, D. (1999): Influence of Additives on the Properties of Spherical Ni Particles Prepared by Ultrasonic Spray Pyrolysis", J.Mater. Res., 14, (7) pp.3059-3065.

61) Cerovic, Lj. Milonjic, S., Zivkovic, Lj., Uskokovic, D. (1996): Synthesis of Spherical b-Silicon Carbide Particles by Ultrasonic Spray Pyrolysis", J.Am.Ceram.Soc., 79, pp.2215-17.

62) Saponjic, Z.V., Rakocevic, Z., Dimitrijevic, N.M., Nedeljkovic, J.M., Jokanovic, V., Uskokovic, D.P (1998): Tailor Made Synthesis of Q-TiO2 Powder by Using Quantum Dots as Building Blocks, Nanostruct. Mater., 10, pp.341-348.

63) Mancic, L., Milosevic, O., Marinkovic, B., da Silva Lopez, M.F., Rizzo, F. (2000): Rapid Formation of High Tc Phase in Bi-Pb-Sr-CaCu-O System, Physica C, 341-348, pp.503-504.

64) Mancic, L., Milosevic, O., Labus, N., Ristic, M. (2001): High Tc Superconducting Powders Synthesis from Aerosol", J.Euro.Ceram.Soc., 21, pp.2765-2769.

65) Wang, Y., Milosevic, O., Gómez, L., Rabanal, M.E., Torralba, J.M., Yang, B., Towsend, P. D. (2006): Thermoluminiscence responses from europium doped gadolinium oxide Journal of Physics: Condensed Matter, 18, pp.9257-9272.

66) Rabanal., M.E, Gómez, L.S, Khalifa, A., Torralba, J.M., Mancic. L., Milosevic, O. (2007): Structural properties of europia-doped-gadolinia synthesized through aerosol, Journal of European Ceramic Society 27 (13-15) pp.4325-4328.

67) Gómez, L. S., Rabanal, M.E., Torralba, J. M., Mancic, L., Milosevic, O. (2007): Structural and morphological study of nanoceramics prepared by spray pyrolysis. Ceramic Transactions, Characterization & Control of interfaces for High Quality Advanced materials. The

American Ceramic Society, eds. Kevin Ewsuk et. al . Vol. 198, pp.193-197

68) Marinkovic, K., Mancic, L., Gomez, L., Rabanal, M.E., Dramicanin, M., Milosevic, O., Nanostructured (Y1-xGdx)2O3:Eu^{3+} powders obtained through aerosol synthesis, ICCCI 2009, Kurashiki, September 6-9th, Japan

69) Marinkovic, K., Mancic, L., Gomez, L.S., Rabanal, M.E., Dramicanin, M., Milosevic, O. (2009): Photoluminescent properties of nanostructured Y2O3:Eu^{3+} powders obtained by aerosol synthesis, ICOM 2009, Herceg Novi, 27-30th August, Montenegro.

70) del Rosario, G., Ohara, S., Mancic, L., Milosevic, O. (2004): Characterisation of YAG:Ce powders thermal treated at different temperatures, Appl. Surf. Sci., 238 (1-4) pp.469-474.

71) Milosevic, O., Mancic, L., Ohara, S., del Rosario, G., Vulic, P. (2004): Aerosol synthesis and phase development in Ce-doped nanophased Ytrrium-aluminium garnet (Y3Al5O12:Ce) particles, Ceramic transactions, Characterisation and Control of Interfaces for High Quality Advanced Materials, eds. K.Ewsuk, K.Nogi, M.Reiterer, A.Tomsia, S.J.Glass, R.Waesche, K.Uematsu, M.Naito, American Ceramic Society, 146, pp.435-441.

72) Mancic, L., del Rosario, G., Marinkovic Stanojevic, Z., Milosevic,O. (2007): Phase evolution in Ce doped yttrium aluminium based particles derived from aerosol, J.Eur.Cer.Soc., 27, pp.4329-4332.

73) Kandic, Lj., Marinkovic, K., Mancic, L., del Rosario, G., Milosevic, O. (2007): Low Temperature Aerosol Synthesis of YAG:Ce^{3+} Nanostructures: Comparative Study of the XRPD Micro structural Parameters, Mat. Sci.Forum, 555, pp.395-400.

74) Mancic, L., Marinkovic, K., Marinkovic, B., Dramicanin, M. and Milosevic, O. (2009): YAG:Ce $^{3+}$ nanostructured particles obtained via spray pyrolysis of polymeric precursor solution, J.Eur.Cer.Soc., in press, doi:10.1016/j.jeurceramsoc.2009.05.037.

75) Jugovic, D., Uskokovic, D. (2009): A review of recent developments in the synthesis procedures of lithium iron phosphate powders, Journal of Power Source, 190, pp.538–544.

76) Rack, P. D. , Holloway, P. H. (1998): The srtructure, device physics and material properties of thin film electroluminescent displays, Mater. Sci. Eng., 4, pp.171-219.

77) Ropp, R. C. (1991): Luminescence and the Solid State, Elsevier Science Publishers B. V., New York.

78) Maghrabi, M., Townsend, P.D., Vazquez, G. (2001) Low temperature luminescence from the near surface region of. Nd:YAG, J. Phys.: Condens. Matter, 13, pp.2497–515.

79) Kang, Y.C., Lenggoro, I.W., Park, S.B. and Okuyama, K. (2000): YAG-Ce phosphor particles prepared by ultrasonic spray pyrolysis, Mater. Res. Bull., 35, pp.789-798.

80) Zych, E., Brecher, C., Wojtowicz, A.J. and Lingertat, H.

(1997): Luminescence properties of Ce-activated YAG optical ceramic scintillator materials, J. Lumin., 75, pp.193-203.

81) Kang., Y. C., Park, S. B., Lenggoro, I.W., Okuyama, K. (1999): Gd2O3:Eu phosphor particles with sphericity, submicron size and nonaggregation characterisitics, Journal Phys. Chem. Solids 60, pp.379-384.

82) Jung, D.S., Hong, S.K., Lee, H. J., Kang, Y.C. (2006): Gd2O3:Eu phosphor particles prepared from spray solution containing boric acid flux and polymer precursor by spray pyrolysis, Opt. Mater., Vol. 28(5) pp.530-535.

83) Pires, A. M., Santos, M.F., Davolos, M.R., Stucchi, E.B. (2002): The effect of Eu^{3+} ion doping concentration in Gd2O3 fine spherical particles, J. Alloy Compd., 344, pp.276-279.

84) Koo, H., Ju, S., Jung, D.S., Hong, S.K., Kim, D.Y., Kang, Y.C. (2006): Morphology Control of Gd2O3:Eu phosphor particles with cubic and monoclinic phases prepared by high temperature spray pyrolysis (2006): Jap. J. Appl. Phys., 45 (6A) pp.5018-5022.

85) Kim, E. J., Kang, Y.C., Park, H.D., Ryu S.K. (2002): UV and VUV characteristics of (YGd)2O3 phosphor particles prepared by spray pyrolysis from polymeric precursors, Mater.Res.Bull., 2159, pp.1-10.

86) Gómez, L. S., Sourty, E., Freitag, B., Milosevic, O., Rabanal, M. E., A three dimensional study of Gadolinium oxides doped with europium formed by aerosol method using electron tomography, to be published.

87) Bae, J.S., Yi, S.S., Kim, J. H., Shim, K.S., Moon, B.K., Jeong, J.H., Kim, Y. S. (2006): Crystalline-phase-dependent red emission behaviours of Gd2O3:Eu^{3+} thin-film phosphors, Applied Physics A , 82, (2) pp.S.369-372.

88) Seo, D.J., Kang, Y.C., Park, S. B. (2003): The synthesis of (Y1-xGdx)2O3:Eu phosphor particles by flame spray pyrolysis with LiCl flux. Appl. Phys. A., 77, pp.659-663.

89) Bhargave, R. N., Gallagher, D., Welker T. (1994): Doped nanocrystals of semiconductors-a new class of luminescent materials J. Lumin., 61, pp.275.

90) Wan, J., Wang, Z., Chen, X., Mu, L., Qian, Y. (2005): Shape tailored photoluminescent intensity of red phosphor Y2O3:Eu^{3+}. Journal of Crystal Growth., 284, pp.538-543.

91) Tissue, B. M. and Yuan, H. B. (2003): Structure, particle size and annealing of gas-phase condensed Eu^{3+}: Y2O3 nanophosphors, J.Solid State Chem., 171, pp.12-18.

92) Allieri, B., Depero, L. E., Marino, A., Sangalleti, L., Caporaso, L., Speghini, A., Bettinelli, M. (2000): Growth and microstructural analysis of nanosized Y2O3 doped with rare-earths, Mater. Chem. Phys., 66, 164-177.

93) Mitric, M., Onnerud, P., Rodic, D., Tellgren, R., Szytula, A., Napijalo, M.Lj. (1993): The preferential site occupation and magnetic properties of GdxY2-xO3, J. Phys.Chem.Solids, 54, 967-972.

94) Dosev, D., Guo, B., Kennedy, I.M. (2006): Photoluminescence of Eu^{3+}: Y2O3 as an indication of crystal struc-

ture and particle size in nanoparticles synthesized by flame spray pyrolysis Aerosol Sci., 37, 402-412.

95) Malta, O, Antic-Fidancev, E., Lemaitre-Blaise, M., Milicic-Tang, A., Taibi, M. (1995): The crystal field strength parameter and the maximum splitting of the $^7F_1$ manifold of the Eu^{3+} ion in oxides, Journal Alloys and Compounds, 228, pp.41-44.

96) Pons Y Moll, O., Huignard, A., Antic-Fidancev, E., Aschehoug, P., Viana, B., Millon, E., Perrière, J., Garapon, C., Mugnier, J. (2000): Eu^{3+}- and Tm^{3+}-doped yttrium oxide thin films for optical applications, Journal of Luminescence, 87-89, pp.1115-1117.

97) Tallant, D.R., Seager, C.H., Simpson, R.L. (2002): Energy transfer and relaxation in europium-activated Y_2O_3 after excitation by ultraviolet photons, Journal of Applied Physics, 91, pp.4053-4064.

98) Andrić, Ž., Dramićanin, M.D., Mitrić, M., Jokanović, V., Bessiere, A., Viana, B. (2008): Polymer complex solution synthesis of $(YxGd1-x)_2O_3$:Eu^{3+} Nanopowders, Optical Materials, 30, pp.1023-1027.

99) Gomez, L. S. (2009): Sintesis y caracterization de oxidos nanoestructurados de gadolinio e ytrio dopados con europio obtenidos mediante el metodo de spray pirolisis, PhD Thesis, University Carlos III, Madrid.

100) Yang, H., Lee, D-K., Kim, Y-S. (2009): Spectral variations of nano-sized $Y_3Al_5O_{12}$:Ce phosphors via codoping/substitution and their white LED characteristics, Materials Chemistry and Physics 114, pp.665-669.

101) Blasse, G., Bril A. (1967): Investigation of some Ce-activated phosphors, Journal of Chemical Physics, , 47(12) pp.5139-5245.

102) Kang, Y.C., Park S.B., and Lenggoro, I.W., Okuyama, K. (1998): Preparation of non aggregation YAG-Ce phosphor particles by spray pyrolysis, Aerosol Sci., 29, pp.S 911-S912.

103) Kang, Y.C., Lenggoro, I.W., Park, S.B., Okuyama, K. (2000): YAG:Ce phosphor particles prepared by ultrasonic spray pyrolysis. Mater. Res. Bull., 35, pp.789–798.

104) Qi, F.X., Wang, H.B., Zhu, XZ. (2005): Spherical YAG: Ce^{3+} Phosphor Particles Prepared by Spray Pyrolysis, Journal of Rare Earths, 23, 4, pp.397-400.

105) Lee, S.H., Jung, D.S., Han, J.M., Koo, H.Y., Kang, Y.C. (2009): Fine-sized $Y_3Al_5O_{12}$:Ce phosphor powders prepared by spray pyrolysis from the spray solution with barium fluoride flux, J. Alloys and Compounds 477, pp.776-779.

106) Purwanto, A., Wang, W.N. Ogi, T, Lenggoro, I.W., Tanabe, E., Okuyama, K. (2008): High luminance YAG: Ce nanoparticles prepared from urea-added aqueous precursor by flame-process, Journal of Alloys and Compounds, 463, (1-2) pp.350-357.

107) Hyun K.J., Lee, W. (2007): Enhanced luminescent properties of $Y_3Al_5O_{12}$:Tb^{3+},Ce^{3+} phosphor prepared by spray pyrolysis, Journal of Luminescence 126, pp.469-474.

108) Ullal, C.K., Balasubramaniam, K.R., Gandhi, A.S., Jaram, V. (2001): Non-equilibrium phase synthesis in Al_2O_3-Y_2O_3 by spray pyrolysis of nitrate precursors, Acta Materialia 49 (14) pp.2691-2699.

109) Nyman, M., Caruso J, HampdenSmith, M.J. (1997): Comparison of solid-state and spray pyrolysis synthesis of yttrium aluminate powders, J.Amer.Ceram.Soc. 80 (5) pp.1231-1238.

110) Marinkovic, K., Mancic, L., Pavlovic, V.B., Dramicanin, M., Milosevic, O. (2008): Urea-assisted self-combustion aerosol synthesis of $Y_3Al_5O_{12}$:Ce^{3+}, YUCOMAT, September 8-12 2008, Herceg Novi, Montenegro, p.139.

Author's short biography

O. Milosevic

Olivera B. Milosevic, Research professor at the Institute of Technical Sciences of Serbian Academy of Sciences and Arts (ITS SASA), Belgrade, Serbia, was born on August 13th 1955. in Belgrade (Serbia). She graduated Chemical engineering at the Faculty for Technology and Metallurgy, Belgrade University and from the same University she received her M.Sc. and D.Sc. degrees in Materials Science. She is awarder of the Japanese Science and Technology Agency Fellowship in 1999, when she joined Japan Fine Ceramic Center, Nagoya, Japan as a Visiting Researcher. She participated as a Visiting Professor at the University Carlos III, Madrid, Spain, Department for Materials Science and Engineering, in 2001, 2002, 2003 and 2005/2006 and is awarder of a one year Sabbatical grant from the Ministry of Science and Education, Madrid, Spain. She is invited as Visiting professor to join JWRI, Osaka University as JSPS fellowship awarder in 2010.

The main field of her scientific work has been related to the advanced materials processing with particular emphasis in research and development of nanophased functional materials (ceramics and composites) using chemical reactions in aerosols. The significance of her researches is confirmed with more than 200 scientific papers in relevant scientific journals and presentations at the International Conferences. Her results have been cited more than 200 times in scientific literature. Most of her work she delivered either as plenary or invited lectures at Hiroshima University, Japan, Konan University, Kobe, Japan, Japan Fine Ceramic Center, Nagoya, Japan, Microcoating Technology, USA etc., Beijing Normal University, China, "Jozef Stefan" Institute, Slovenia, Osaka University, Japan etc. She currently leads the research activities focused to the innovative processing methods for 1D and 3D nanoscaled functional materials. Dr. Olivera B. Milosevic is a full member of the International Institute for the Science of Sintering (IISS) and the Engineering Academy of Serbia, a member of the European Microscopic Society, Serbian Chemical Society and Serbian Crystallographic Society.

L. Mancic

Lidija Mancic was born on August 18th 1968 in Zajecar, Serbia. She received her BSc (1992) and M.Sc. (1996) degrees at Belgrade University, Technical faculty in Bor – Inorganic Chemistry Department, and D.Sc. (2004) in the field of Materials Science at the Centre for Multidisciplinary Studies, Belgrade University. Since 1996 she has worked in ITS SASA on the synthesis and characterization of superconductors and semiconductors (ultra-dispersed and nano-powders, bulk and films using chemical reactions in aerosols). Since 2006 she has been engaged in research devoted to one-dimensional nanomaterials processing through hydrothermal route at Pontificia Universidade Catolica do Rio de Janeiro within the framework of her post-doc studies. She is a reviewer for several peer reviewed journals in the area of material science.

M. E. Rabanal

Maria Eugenia Rabanal was born on March 12th, 1969 in Madrid, Spain. She received her BSc (1993) and Master (1996) degrees at the University Complutense in Madrid, Spain in the field of Physical Chemistry. In 2002 she received her Ph.D. in Materials Science at the University Carlos III, Madrid, Spain, working on soft magnetic materials and high energy mechanical milling process. She was a pre-doctoral fellow along the course 1999/2000 at the Physics Department in the Trinity College in Dublin. She got a position in 1998 as an Assistant professor at Department of Materials Science and Engineering and Chemistry Engineering of the University Carlos III of Madrid, Spain where she has presently the permanent position as a lecturer. Her current research activities are focused on structural, morphological and functional characterization of advanced materials using a variety of experimental techniques. She has more than 60 publications in international journals and communications at International Conferences.

L. S. Gomez

Luz Stella Gómez Villalba was born on May 26th 1963 in Columbia. She received her BSc (1988) at the National University of Columbia in the field of geology and her PhD (2008) in the field of Materials Science at the University Carlos III, Materials Science and Engineering Deptartment, Madrid, Spain. In the period from 1988-2001 she was engaged at INGEOMINAS, Colombian Institute of Researchers in geology, mining and chemistry (Colombia) where she conducted research work in the field of petrology and mineralogy. She is presently engaged at ECONOMIC GEOLOGY INSTITUTE- Superior Council of Scientific Researchers (CSIC)- Universidad Complutense de Madrid (Madrid- Spain) where she realized researches in nanotechnology applied to geomaterials in cultural heritage conservation. Her current research interest includes the structural characterization of nanophase materials with expertise in the field of Transmission Electron Microscopy and XRD powder diffraction.

K. Marinkovic

Katarina Marinkovic was born on March 11th, 1978 in Belgrade, Serbia. She received her BSc in Chemical Engineering in 2003, and M.Sc. in Material Science in April 2009, both at the Faculty of Technology and Metallurgy, Belgrade University, Serbia. She works as a research assistant in ITS SASA since 2006. in the area of conducted synthesis of nanostructured powders and thin films through aerosol methods. Within COST 539 Action she got a one month Short Term Scientific Mission (STSM) at the University Carlos III, Madrid, Spain, November-December 2006. She has published several papers in peer reviewed journals and presentations at international Conferences.